scientific reports

Check for updates

OPEN

Prognostic and therapeutic relevance of IL2RG-related LncRNAs in clear cell renal cell carcinoma

Weijing Hu[1,6], Bo Wu[2,6], Yongquan Chen[3], Xiaoling Guo[4], Xiaosong Wang[1] & Dongwen Wang[1,5]✉

Interleukin-2 Receptor Subunit Gamma (IL2RG) has been implicated in various cancers, but its role in clear cell renal cell carcinoma (ccRCC) remains unclear. This study aimed to explore IL2RG expression, its relationship with IL2RG -related lncRNAs (IRLs). Gene expression and clinical data for ccRCC were obtained from The Cancer Genome Atlas (TCGA) and the Gene Expression Omnibus(GEO) database. The IRL signature was constructed using Least Absolute Shrinkage and Selection Operator (LASSO) regression analysis. Clinical data validated the diagnostic value of the signature. The prognostic value of the signal was assessed using Kaplan-Meier analysis and Receiver Operating Characteristic (ROC) curves. The prognostic value of the nomogram was further evaluated through calibration curves, ROC curves, and Decision Curve Analysis (DCA). Gene set enrichment analysis (GSEA), single-sample GSEA (ssGSEA), CIBERSORT algorithms, and TISCH2 database were applied to analyze immune function and immune cell infiltration in different risk groups. Clinical treatment differences among populations with varying risks and susceptibilities were predicted using R packages. The expression of IL2RG and key lncRNAs was validated by quantitative real-time polymerase chain reaction (qRT-PCR) and immunohistochemistry (IHC). IL2RG was significantly upregulated in ccRCC tissues and correlated with advanced clinical stages ($p < 0.001$). High IL2RG expression was linked to worse overall survival (OS), disease-specific survival (DSS), and progression-free interval (PFI) ($p < 0.05$). A 6-IRLs signature was identified, and the resulting model accurately predicted survival outcomes. Immune-related pathways were enriched in high-risk patients, and drug sensitivity analysis indicated that high-risk patients were more responsive to sunitinib and temsirolimus. IL2RG and its related 6-IRLs are potential biomarkers for ccRCC progression. The 6-IRLs model provides a robust tool for predicting prognosis and guiding therapeutic decisions.

Keywords Clear cell renal cell carcinoma (ccRCC), Interleukin-2 Receptor Subunit Gamma (IL2RG), Long non-coding RNAs (lncRNAs), Biomarkers, Immune response, Tumor microenvironment (TME)

Renal cell carcinoma (RCC) is a highly malignant tumor originating from the renal tubular epithelium system[1]. In developed countries, the annual incidence of RCC continues to rise[2]. Clear cell renal cell carcinoma (ccRCC) is the most prevalent subtype, accounting for approximately 70–80% of all renal cancer cases[3]. It is notorious for its aggressive behavior and high metastatic potential, making treatment and management particularly challenging[4]. Clinically, ccRCC is often diagnosed at an advanced stage due to the lack of overt symptoms in its early phases. Treatment options for ccRCC include surgical interventions such as radical nephrectomy[5]. However, advanced or metastatic ccRCC often precludes surgical options, necessitating targeted therapies, immunotherapies, or a combination of both. Yet, the tumor microenvironment is characterized by significant immune suppression, leading to poor prognoses[6]. Therefore, unraveling the complex molecular mechanisms underlying ccRCC,

[1]Shanxi Medical University, Taiyuan 030001, Shanxi, China. [2]Department of Urology, First Hospital of Shanxi Medical University, Taiyuan 030001, Shanxi, China. [3]Department of Urology, Shanxi Coal Center Hospital, Taiyuan 030001, Shanxi, China. [4]Geriatrics Department, Xi'an Central Hospital, Xi'an 710003, China. [5]National Cancer Center/National Clinical Research Center for Cancer/Cancer Hospital & Shenzhen Hospital, Chinese Academy of Medical Sciences and Peking Union Medical College, Shenzhen 518116, Guangdong, China. [6]Weijing Hu and Bo Wu contributed equally to this work. ✉email: Urology2007@126.com

identifying novel biomarkers for early detection, and exploring new therapeutic targets to enhance treatment efficacy and overcome resistance are pressing issues.

Interleukin-2 Receptor Subunit Gamma (IL2RG) is a pivotal immune-related gene that encodes the γ subunit of the interleukin-2 receptor[7]. This receptor is a central component of several cytokine receptor complexes, including IL-2, IL-4, IL-7, IL-9, IL-15, and IL-21[8]. The IL2RG gene is located on the X chromosome, and its mutations are known to be associated with immunodeficiency disorders such as severe combined immunodeficiency (SCID), underscoring its crucial role in the normal functioning of the immune system[9]. In recent years, IL2RG has been identified as playing a significant role within the tumor microenvironment (TME)[10]. The TME refers to the internal environment in which tumor cells exist, comprising not only the tumor cells themselves but also microvasculature, immune cells, stromal cells, secreted signaling molecules, and extracellular matrix components[11]. The TME of ccRCC is abundant in immune cells, including T cells, B cells, and natural killer (NK) cells, whose function and distribution profoundly influence tumor progression and therapeutic response. These cells are also involved in antitumor immune responses and the mechanisms of immune evasion[12]. IL2RG may modulate the immune status of the TME by affecting the development and function of immune cells.

For instance, in breast cancer research, the expression levels of IL2RG have been found to closely correlate with immune cell infiltration within the tumor[13]. The downregulation or functional loss of IL2RG may lead to the suppression of T cell activity, thereby disrupting the immune equilibrium in the tumor microenvironment and rendering tumor cells more adept at evading immune surveillance[14]. Moreover, the interaction between IL2RG and the IL-15 signaling pathway is considered a crucial mechanism in regulating NK cell function within the TME, influencing both tumor progression and prognosis[15]. Additionally, IL2RG has emerged as a potential target in the field of immunotherapy for ccRCC. Several studies have investigated its application in immune checkpoint inhibitors and other immunotherapeutic strategies, revealing that IL2RG may serve as a biomarker for predicting treatment efficacy and patient outcomes[16]. Given its pivotal role in modulating immune cell function and maintaining immune homeostasis, research into IL2RG holds significant clinical importance. Further exploration of the interplay between IL2RG and the TME in ccRCC not only sheds light on tumor immune mechanisms but also presents potential targets for the development of novel immunotherapeutic strategies. Therefore, studying the role of IL2RG in ccRCC is of paramount importance in advancing personalized immunotherapy.

Long non-coding RNAs (lncRNAs) are RNA molecules exceeding 200 nucleotides in length that perform a wide range of cellular functions. While they do not encode proteins, they are deeply involved in regulating gene expression[17]. lncRNAs can influence gene transcription and post-transcriptional processes through various mechanisms, such as acting as 'molecular sponges' for miRNAs, altering chromatin states, and modulating mRNA stability[18]. In recent years, lncRNAs have been found to play pivotal roles in the onset and progression of numerous diseases, particularly in cancer and immune system disorders[19]. The role of the IL2RG gene in the immune system has been extensively studied, demonstrating its crucial regulatory functions in immunodeficiency disorders[10]. In ccRCC, lncRNAs have been implicated in regulating key oncogenes and tumor suppressor genes, influencing tumor proliferation, metastasis, and immune evasion[20]. Specifically, lncRNAs can modulate the expression of immune-related genes within the TME, thereby impacting immune cell function and tumor progression[21]. Given the critical role of IL2RG in immune regulation, it is plausible that lncRNAs may regulate IL2RG expression or function, either directly by interacting with its mRNA or indirectly through signaling pathways that influence immune cell activity in the TME. For example, studies in other cancers, such as colorectal cancer, have shown that lncRNAs may regulate IL2RG expression, potentially influencing tumor progression, by acting as competing endogenous RNAs (ceRNAs)[22]. This suggests a potential regulatory link between IL2RG and lncRNAs in ccRCC, which warrants further investigation to uncover novel molecular mechanisms and therapeutic targets.

In this study, we first employed bioinformatics analysis using R software to examine the The Cancer Genome Atlas Kidney Renal Clear Cell Carcinoma (TCGA-KIRC) database, investigating the expression differences of the IL2RG gene between ccRCC and normal tissues, as well as its correlation with clinicopathological features and prognosis. Subsequently, we assessed the mRNA and protein expression levels of IL2RG in ccRCC and adjacent normal tissues through Quantitative real-time polymerase chain reaction(qRT-PCR) and Immunohistochemistry (IHC) experiments. Finally, we developed a signature comprising 6 IL2RG-related lncRNAs (IRLs) and evaluated its diagnostic, prognostic, and therapeutic value for ccRCC. Key lncRNAs were further validated using qRT-PCR. The results indicate that this signature holds significant potential for clinical application, providing guidance for precise diagnosis and offering new perspectives on immunotherapy for ccRCC.

Materials and methods

Data acquisition, processing, and clinical sample collection

IL2RG pan-cancer analysis was conducted using the GEPIA2 database[23] (http://gepia2.cancer-pku.cn/). TCGA datasets were obtained from The Cancer Genome Atlas (TCGA) database[24]and the transcriptomic gene expression matrix from the TCGA-KIRC project was downloaded and organized in transcripts per million (TPM) format. This dataset includes RNA sequencing (RNA-seq) data from 533 ccRCC tissues and 72 normal kidney tissues. The inclusion criteria were as follows: ① the kidney as the primary site of disease; ② availability of complete lncRNA sequencing data and clinical information for the patients. Logarithmic transformation of the gene expression matrix data was performed to achieve normalization. We utilized the "limma" package[25] in R software to correct the downloaded gene expression matrix. Tumors were classified according to the TNM staging system into stages I through IV, reflecting tumor size and spread. Based on the International Society of

Urological Pathology (ISUP) grading system, tumors were graded from 1 to 4 (G1 to G4), indicating increasing levels of malignancy. Samples with insufficient details were excluded.

Fifty specimens were collected between January 2023 and October 2023 from the Department of Urology at the First Hospital of Shanxi Medical University, where patients underwent radical nephrectomy. Tissue samples from patients pathologically diagnosed with ccRCC, along with adjacent non-cancerous tissues, were used as the study subjects. Exclusion criteria included any preoperative tumor-suppressive treatments, such as radiotherapy or chemotherapy, and incomplete clinical information. Immediately after excision, the specimens were immersed in liquid nitrogen and subsequently stored in an ultra-low temperature freezer at – 80 °C. A total of 50 specimens were included in this study.The study was conducted in accordance with the Declaration of Helsinki, and approved by the Ethics Committee of the First Hospital of Shanxi Medical University (No. 2021K034,2021-04-26).

Analysis of the clinical correlations of IL2RG expression

To identify the differential expression levels of IL2RG in ccRCC tissues compared to normal kidney tissues, the "limma" package[25] in R software was employed. $P<0.05$ was considered statistically significant. The R packages "pheatmap" and "boxplot" were utilized to display the expression levels and differences of IL2RG, while the "survival" package was used to assess the prognostic value of the IL2RG gene, with prognostic outcomes including Overall Survival (OS), Disease-Specific Survival (DSS), and Progression-Free Interval (PFI).

Screening of potential regulatory IRLs

Given the strong association between IL2RG and immunity, we first retrieved 3,178 immune-related genes from the Immport database[26] (https://www.immport.org/) and the InnateDB database[27] (https://www.innatedb.ca/). We then conducted a Pearson correlation analysis to identify genes associated with IL2RG ($r>0.8$ and $P<0.001$) and intersected these with the retrieved genes, yielding 26 immune genes strongly correlated with IL2RG. Subsequently, we performed Pearson correlation analysis to identify lncRNAs co-expressed with these IL2RG-related genes ($r>0.5$ and $P<0.001$). Using these IL2RG-co-expressed lncRNAs, we employed the "limma" package to analyze differential expression of lncRNAs between 72 normal kidney tissues and 533 ccRCC tissues. We conducted a co-clustering analysis to categorize the IRLs. Clustering was performed using the "limma"[25] and "ConsensusClusterPlus" packages[28] with results visualized through "survminer," "survival," and "pheatmap" packages, including survival curves and heatmaps of clinical-pathological features (age, gender, metastasis, and histological malignancy).

Construction of the IRLs signature

To establish a robust prognostic model, we randomly divided 530 ccRCC patients with survival data into training and testing cohorts at a 1:1 ratio, with the features listed in Table 1. We constructed an lncRNA risk score formula using least absolute shrinkage and selection operator (LASSO) regression analysis and selected the optimal λ with the minimal bias in partial likelihood to determine the most suitable genes. The formula is as follows: Risk Score = Σ (Exp[lncRNA] × coef[lncRNA]), where coef[lncRNA] denotes the regression coefficient and Exp[lncRNA] reflects the expression level of the corresponding lncRNA. Each sample was classified into high-risk or low-risk groups based on the median risk score. An IRLs prognostic model was established using the TCGA-KIRC training set, and a correlation heatmap was generated. Validation was performed in both the internal testing set and the entire TCGA-KIRC cohort.

To further assess the generalizability of the signature, we additionally validated its prognostic performance in an independent external cohort (GSE167573) from the Gene Expression Omnibus (GEO) database. Risk scores for the external samples were calculated using the same formula derived from the TCGA training set, and survival analysis was conducted accordingly, with $P<0.05$ indicating statistical significance.

Evaluation of the prognostic model's efficacy and clinical value

Using the median risk score of each sample as a threshold, the samples were categorized into low-risk and high-risk groups, and the OS between these groups was compared using the log-rank test. Principal Component Analysis (PCA) was employed to assess the clustering capability of the IRL model risk scores. Combining risk scores with clinical data such as age, sex, tumor grade, and stage of ccRCC patients, Cox regression analysis was performed to determine whether the model could serve as an independent prognostic factor.

Construction of a nomogram

To construct the prognostic nomogram, we first selected key features from clinical data, such as age, gender, tumor stage, and grade, using Cox proportional hazards regression analysis, along with six lncRNA biomarkers that were significantly associated with patient prognosis in univariate analysis. The coefficients of the clinical and lncRNA features in the regression model reflected their impact on patient prognosis. The weight of each feature was calculated based on its regression coefficient, and scores were assigned accordingly. In the nomogram, each variable was given a score, and the total score was used to predict the patient's prognostic risk.We constructed a nomogram using the "rms" package in R software to predict the survival rates of ccRCC patients at 1, 3, and 5 years. The reliability and accuracy of the nomogram were assessed through calibration curves, Receiver Operating Characteristic (ROC) curves, and Decision Curve Analysis (DCA).

The relationship between the IRLs model risk score and immune analysis

To investigate the pathway differences between high-risk and low-risk groups, Kyoto Encyclopedia of Genes and Genomes[29] (KEGG) pathway enrichment analysis[30] was performed based on risk scores, employing Gene Set Enrichment Analysis (GSEA)[31]. In R software, we utilized the "GSVA" package[32] to compute the activity of

Characteristic	Training cohort (*N* = 266)	Testing cohort (*N* = 264)	TCGA cohort (*N* = 530)
Age (years), n (%)			
≤ 65	182 (68.4%)	178 (67.4%)	360 (67.9%)
> 65	84 (31.6%)	86 (32.6%)	170 (32.1%)
Gender, n (%)			
Female	98 (36.8%)	88 (33.3%)	186 (35.1%)
Male	168 (63.2%)	176 (66.7%)	344 (64.9%)
Grade, n (%)			
G1-2	122 (45.9%)	119 (45.1%)	241 (45.5%)
G3-4	140 (52.6%)	141 (53.4%)	281 (53.1%)
Unknown	4 (1.5%)	4 (1.5%)	8 (1.5%)
Stage, n (%)			
Stage I–II	168 (63.2%)	154 (58.3%)	322 (64.1%)
Stage III–IV	95 (35.7%)	110 (41.7%)	205 (38.7%)
Unknown	3 (1.1%)	0 (0%)	3 (0.5%)
T stage, n (%)			
T1–2	178 (66.9%)	162 (61.4%)	340 (64.2%)
T3–4	88 (33.1%)	102 (38.6%)	190 (35.8%)
M stage, n (%)			
M0	211 (79.3%)	209 (79.2%)	420 (79.2%)
M1	41 (15.4%)	37 (14.0%)	78 (14.7%)
Unknown	14 (5.3%)	18 (6.8%)	32 (6.0%)
N stage, n (%)			
N0	113 (42.5%)	126 (47.7%)	239 (45.1%)
N1	10 (3.8%)	6 (2.3%)	16 (3.0%)
Unknown	143 (53.8%)	132 (50.0%)	275 (51.9%)

Table 1. Clinical characteristics included in this study from the TCGA database. *TCGA*:The Cancer Genome Atlas.

13 immune-related pathways through single-sample GSEA (ssGSEA)[31]. Immune scoring, including ESTIMATE score[33] immune score, and stromal score, was conducted to assess variations in immune infiltration levels between the groups. The CIBERSORT algorithm was employed to calculate immune cell infiltration levels, and Pearson correlation analysis was used to explore the relationship between risk scores and immune cell infiltration levels. Furthermore, to investigate the cell-type–specific distribution of the 6-IRLs in the tumor microenvironment, we analyzed their expression profiles in ccRCC-related datasets using the Tumor Immune Single-cell Hub 2 (TISCH2) database (http://tisch.compbio.cn/home)[34].

The relationship between IRLs model risk scores and drug sensitivity

Based on the constructed scoring model, we employed the "pRRophetic" package[35] in R to predict the half-maximal inhibitory concentration (IC50) of targeted drugs commonly used in the treatment of ccRCC. These drugs include Sunitinib, Temsirolimus, Sorafenib, Pazopanib, Axitinib.Subsequently, we visualized the drug sensitivity data using the "ggplot2" package and compared the IC50 values between the high-risk and low-risk groups using the two-sample Wilcoxon test to evaluate the correlation between drug sensitivity and risk scores. Statistical significance was set at $P < 0.05$.

Cell culture

Human renal epithelial cells (293T) and human ccRCC cells (786O, 769P, ACHN) were purchased from the Shanghai Cell Bank of the Institute of Life Sciences. These cells were cultured in DMEM (Procell, China) supplemented with 10% fetal bovine serum (Gibco, USA) and 1% penicillin/streptomycin (Solarbio, China). All cells were maintained at 37 °C in a 5% CO_2 incubator and kept at 80%-90% confluence. The culture medium was changed every 2–3 days to ensure optimal cell growth.

Quantitative real-time polymerase chain reaction (qRT-PCR)

The tissue samples were stored in a cryogenic freezer.Total RNA was extracted from frozen tissue samples using TRIzol reagent (TransGen Biotech, Beijing, China) according to the manufacturer's instructions.First-Strand cDNA for qPCR was prepared according to the manufacturer's instructions, and subsequent qPCR reactions were conducted using the appropriate kits. Specifically, the First-Strand cDNA Synthesis SuperMix for qPCR kit and the Green qPCR SuperMix kit were both procured from TransGen Biotech (Beijing, China).GAPDH was used as an internal control, The primer sequences are shown in Table 2.The Gene expression levels were calculated using the $2^{\wedge\text{-}\Delta\Delta Ct}$ method.

Gene name	Forward Primer(5′→3′)	Reverse Primer(5′→3′)
GAPDH	GCTCTCTGCTCCTCCTGTTC	ACGACCAAATCCGTTGACTC
IL2RG	GTGCAGCCACTATCTATTCTCTG	GTGAAGTGTTAGGTTCTCTGGAG
LINC00944	GTGGAGAAGATGAGGAAACTGAGGAA	AAGGGATGATGGAAATAAGCAAGAAG
AC016773.2	TCAGTCCTCCAACTTTGTTCTTCTCC	CACACTTACCTCTTCCTCCACTCCAC
LINC02446	ACATAAGGTGTAAACCAAGTAACCAA	CCAAAAATAAGAAAAGAGTAAAAAAA
LINC02328	TGTGGAAAGTAGTTTGGCGATTTGTC	TGGATTCTGTATTAGGGTATGGGCTC
U62317.2	TTTCTGGATTGTAGTTCTAATTGGGT	TGTTTTTGAGTTGTTATCATTTGCCT
KIF1C-AS1	CCTCAATCTGCGACACATCTTCTACC	TCTAACCCTCCTTCTGCTCTTCCTTT

Table 2. Primer sequences used for qRT-PCR analysis.

Immunohistochemistry (IHC)

The tissues were processed through paraffin embedding, sectioning, deparaffinization, rehydration, antigen retrieval, and endogenous peroxidase blocking. Subsequently, the sections were stained with IL2RG antibody (abcam, USA) diluted to 1:300, followed by a secondary antibody. Color development was achieved using diaminobenzidine (DAB), and counterstaining was performed with hematoxylin to assess the protein expression of IL2RG.

Statistical analysis

Statistical analyses were conducted using R software (version 4.1.3) and GraphPad Prism (version 9.0). The two-sample Wilcoxon rank-sum test was employed to evaluate differences in the expression of IL2RG mRNA and its associated lncRNAs. Univariate Cox regression analysis was utilized to determine the prognostic value of key genes and lncRNAs. LASSO regression analysis was applied to identify crucial lncRNAs associated with IL2RG, and Pearson correlation tests were conducted to explore the relationships among clinical features, risk scores, immune checkpoint inhibitors, and immune infiltration levels. Survival analysis was performed using the Kaplan-Meier method. Inter-group differences were assessed using t-tests, while variance analysis was used to compare differences among three or more groups. Statistical significance was set at $P<0.05$ (*: $P<0.05$, **: $P<0.01$, ***: $P<0.001$).

Results

The expression levels of IL2RG and their relationship with the clinical and pathological characteristics

First, we conducted a pan-cancer analysis of IL2RG and found that IL2RG expression was dysregulated in the majority of cancers. Specifically, IL2RG was upregulated in BRCA, CHOL, HNSC, KIRC, PCPG, and STAD, and downregulated in COAD, KICH, LUAD, and LUSC (Fig. 1A). The varied expression profile of IL2RG across different tumors suggests its involvement in tumorigenesis and progression through distinct mechanisms.

Subsequently, we analyzed the expression of IL2RG in ccRCC concerning its clinical and pathological relevance. We observed that IL2RG expression levels were significantly associated with T stage, N stage, M stage, AJCC stage, and WHO/ISUP grade ($P<0.001$). Moreover, logistic regression analysis revealed a positive correlation between IL2RG expression and ccRCC progression (Fig. 1B–D), though no association was found with age or gender (Fig. S1). Kaplan–Meier survival analysis indicated that high IL2RG expression was correlated with poorer OS, DSS, and PFI ($P<0.05$, Fig. 1E–I).

Using qRT-PCR, we assessed IL2RG mRNA expression in samples ($n=50$) and cell lines, with results presented as $2^{-\Delta\Delta Ct}$. We then performed IHC to examine IL2RG protein expression in ccRCC tissues. The results demonstrated that IL2RG mRNA expression was significantly higher in ccRCC tissues compared to normal tissues ($P<0.05$, Fig. 2A). Similarly, IL2RG mRNA levels in 786O, 769P, and ACHN cells were significantly elevated compared to 293T cells (Fig. 2B). IHC results further revealed that IL2RG protein was predominantly localized in the cell membrane and cytoplasm of ccRCC cells (Fig. 2C), and its expression was significantly higher in ccRCC tissues compared to normal tissues ($P<0.0001$, Fig. 2D).

These findings suggest that IL2RG may play a role in ccRCC tumor progression and could serve as a potential prognostic biomarker for ccRCC patients.

Critical IRLs screening

Through the ImmPort and InnateDB databases, we identified 3178 immune-related genes in humans, and using Pearson correlation analysis, we filtered 67 genes that were highly correlated with IL2RG ($r>0.8$, $P<0.001$) (Table S1). Ultimately, 26 immune genes significantly associated with IL2RG were confirmed (Fig. S2A). The results revealed that IL2RG-related immune genes were generally dysregulated in ccRCC (Fig. S2B). We further generated a heatmap, visually demonstrating the upregulation of these 26 genes in ccRCC tissues (Fig. S2C), suggesting that these genes may play pivotal roles in the initiation and progression of ccRCC.

Subsequently, we continued with Pearson correlation analysis to explore the association between these genes and lncRNAs ($r>0.8$, $P<0.001$), identifying key lncRNAs co-expressed with IL2RG and associated with prognosis (Fig. 3A). The analysis revealed 63 IRLs that were closely related to patient survival outcomes and showed statistical significance (Table S2). We then constructed a forest plot for the top 20 lncRNAs positively correlated with prognosis (Fig. 3B). Through the creation of heatmaps and differential expression plots, we

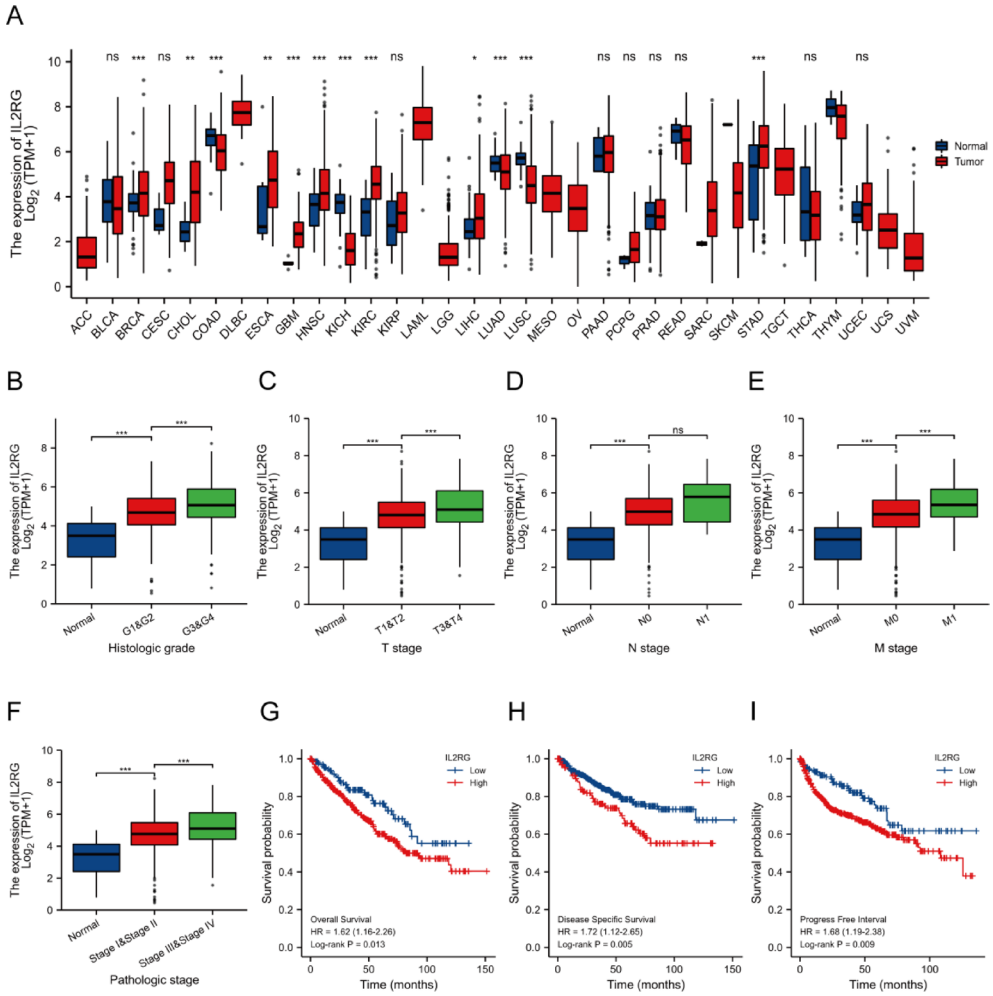

Fig. 1. Pan-cancer analysis of the IL2RG expression and its relationship with clinical characteristics in the TCGA database. (**A**) Pan-cancer analysis; (**B**–**F**) IL2RG mRNA expression vs. histologic grade, T stage, N stage, M stage, and pathologic stage; (**G**–**I**). Correlation between IL2RG expression and overall survival (OS), disease-specific survival (DSS), and progression-free interval (PFI). (*$P<0.05$; **$P<0.01$; ***$P<0.001$; ****$P<0.0001$). IL2RG: Interleukin-2 Receptor Subunit Gamma; TCGA: The Cancer Genome Atlas.

filtered the top 20 lncRNAs most strongly associated with survival and prognosis. The results demonstrated significant differences in the expression of these lncRNAs between groups (Fig. 3C, D).

Consensus clustering based on IRLs

Based on the expression profiles of the 63 key IRLs, we performed consensus clustering analysis[28] on 530 ccRCC patients. Furthermore, the IRL model was constructed with guidance from a consensus clustering analysis, this clustering strategy aimed to simplify clinical testing by selecting a model with a relatively small number of lncRNAs while ensuring robust performance.The results indicated that when k = 2, the cumulative distribution function (CDF) value was relatively low (Fig. 4A, B). Subsequently, we analyzed the correlation between the clustering results and clinical characteristics, revealing significant associations between different clusters and several clinical parameters, including TNM stage, histological grade of malignancy, and clinical staging (Fig. 4C). Further analysis demonstrated that there were significant differences in prognosis among the patient clusters ($P<0.001$, Fig. 4D). Moreover, using the CIBERSORT algorithm, we assessed the immune cell infiltration status of each group and found notable differences in the infiltration levels of B cells, CD8 + T cells, resting CD4 + memory T cells, monocytes, and M2 macrophages between the clusters (Fig. 4E). The ESTIMATE algorithm was further applied to analyze the tumor microenvironment, revealing significant differences in immune scores and microenvironment scores between the clusters ($P<0.001$), although no significant difference was observed in stromal scores between the two clusters (Fig. 4F). Collectively, these findings suggest that clustering based on key IRLs is closely related to patients' clinical characteristics and prognosis, offering potential novel biomarkers for the clinical diagnosis and prognostic evaluation of ccRCC, warranting further investigation.

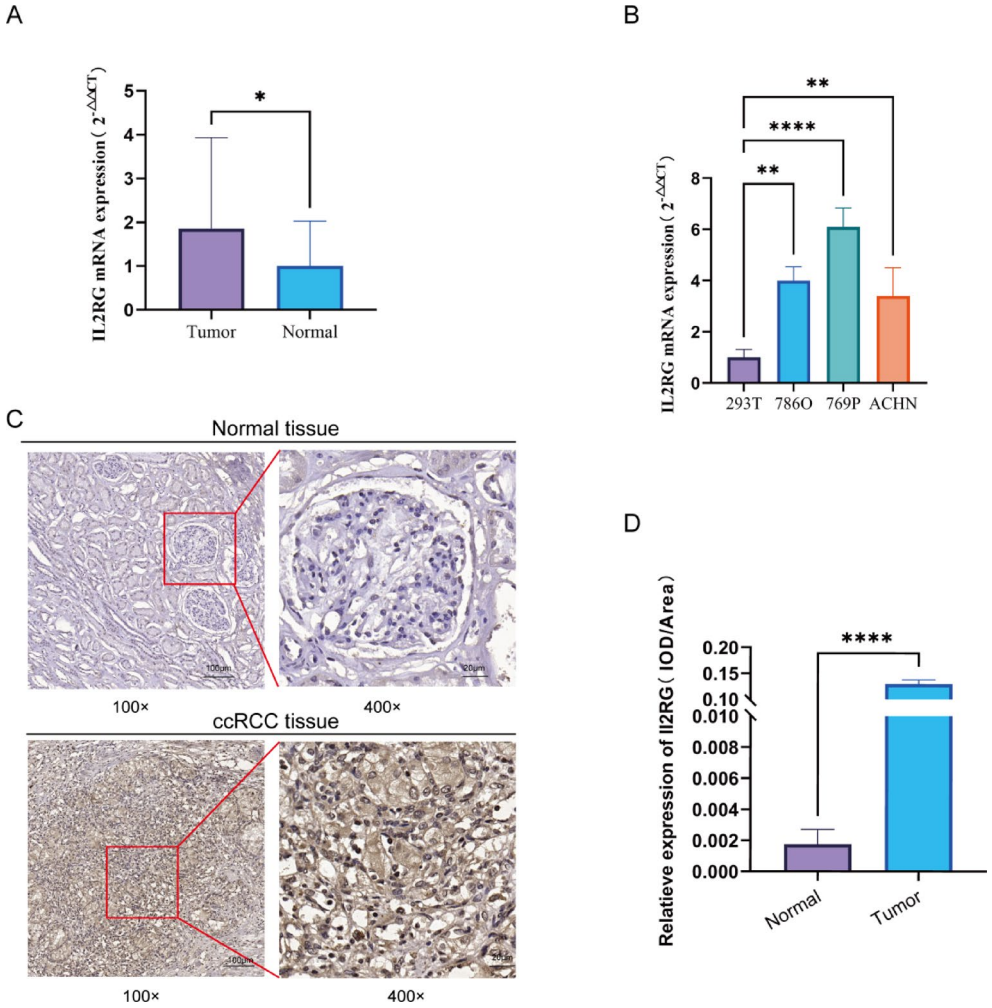

Fig. 2. Tissue validation of IL2RG expression. (**A**) qRT-PCR assessment of IL2RG mRNA expression in ccRCC tissues compared to normal tissues ($n = 50$); (**B**) qRT-PCR evaluation of IL2RG mRNA expression in ccRCC cell lines versus normal cell lines; (**C**, **D**) IHC assessment of IL2RG expression and localization in ccRCC and normal tissues. (*,$P < 0.05$;**,$P < 0.01$;***,$P < 0.001$;****,$P < 0.0001$). ccRCC, Clear Cell Renal Cell Carcinoma; IHC, Immunohistochemical.

Development of a prognostic model based on IRLs

In this study, 530 ccRCC patients were randomly divided into a training cohort (266 cases) and a testing cohort (264 cases). We performed LASSO regression analysis on the 63 IRLs, constructing a prognostic model comprising 6-IRLs (Fig. 5A–C). The formula for calculating the risk score of the model is: Risk score = (LINC00944 × 0.066) + (AC016773.2 × 0.100) + (LINC02446 × 0.002) + (LINC02328 × 0.018) + (U62317.2 × 0.001) + (KIF1C-AS1 × 0.041). We then plotted the forest plots of univariate and multivariate Cox regression analyses for these 6-IRLs (Fig. S3). Using this formula, we calculated each patient's risk score and categorized them into low-risk and high-risk groups based on the median risk score. Survival analysis of the total cohort, training set, and validation set revealed that the survival time of the high-risk group was significantly shorter than that of the low-risk group (Fig. 5D–F), with this difference being statistically significant ($P < 0.05$). Furthermore, ROC curve analysis demonstrated that the 6-IRL model exhibited high accuracy in predicting survival rates (Fig. 5G–I). Survival status curves and scatter plots indicated that as the risk score increased, patient survival time significantly decreased (Fig. 5J–L). t-SNE analysis also revealed a marked distinction between the high-risk and low-risk groups (Fig. 5M–O). To further evaluate the generalizability of our model, we performed external validation using the GSE167573 dataset from the GEO database ($n = 54$). Notably, Kaplan-Meier survival analysis revealed a trend toward poorer survival in the high-risk group, although the difference did not reach statistical significance ($P = 0.065$). This result confirms that the signature retains a degree of applicability in external populations (Fig. S4).

Subsequently, we analyzed the expression of the risk score in ccRCC based on clinical and pathological data from the TCGA database (Fig. 6A). We found that the risk score was significantly associated with T stage, M stage, AJCC stage, and WHO/ISUP grade, with higher risk scores correlating with more advanced T stage, M stage, AJCC stage, and WHO/ISUP grade (Fig. 6B–E) ($P < 0.05$), while no correlation was found with age,

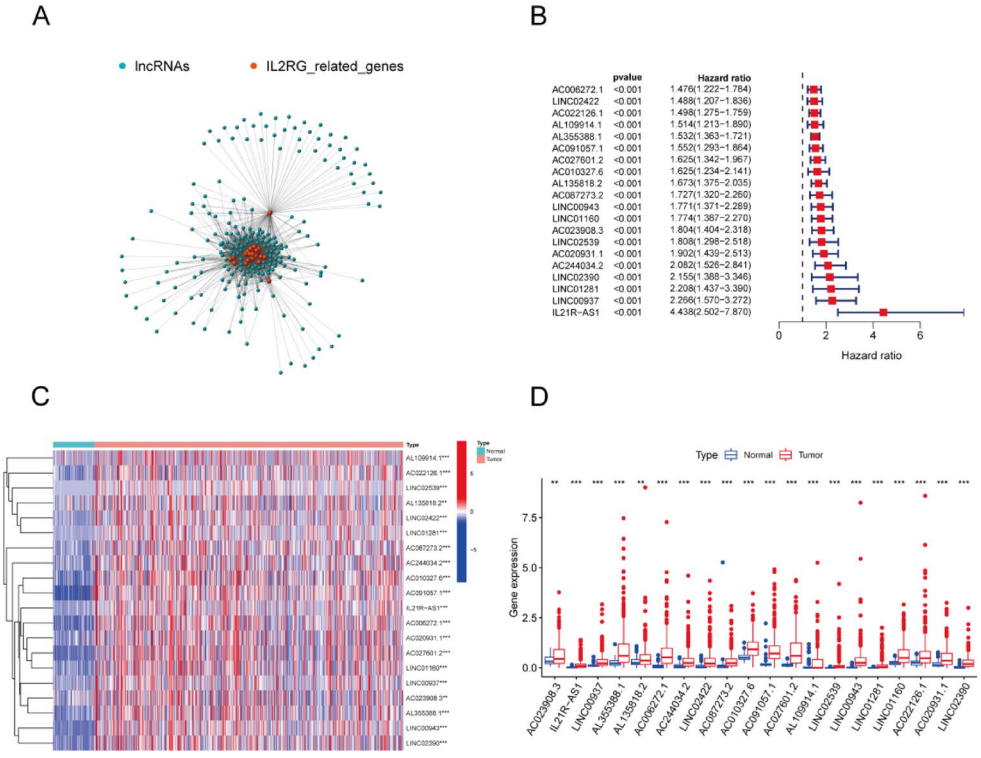

Fig. 3. Screening of key lncRNAs co-expressed with IL2RG. (**A**) The network diagram of key lncRNAs and IL2RG; (**B**) The forest plot of the top 20 lncRNAs positively associated with prognosis; (**C**, **D**). The expression of the top 20 lncRNAs. (**,$P<0.01$; ***,$P<0.001$).

gender, or N stage (Fig. S5). Univariate and multivariate Cox regression analyses indicated that the 6-IRLs model could serve as an independent prognostic factor, with the results supported by both the validation set and the total TCGA cohort (Fig. S6). This suggests that the scoring model holds promise as a crucial indicator for clinical prognostic assessment in ccRCC patients.

The stratified prognostic value of the 6-IRL signature

We further evaluated the prognostic predictive capability of the 6-IRLs signature across various clinical strata, including gender (female vs. male), age (≤65 years vs. >65 years), AJCC stage (I–II vs. III–IV), ISUP grade (I–II vs. III–IV), T stage (T1–2 vs. T3–4), M stage (M0 vs. M1), and N stage (N0 vs. N1). The results revealed a significant difference in survival prognosis between high-risk and low-risk patients in most clinical groups, with high-risk patients exhibiting notably poorer outcomes (Fig. 7). However, in subgroups of patients aged >65 years, with ISUP grade I–II, M1, and N1, the survival differences were not statistically significant (Figure S7).

Development and validation of the prognostic nomogram

We integrated multiple clinical factors closely associated with patient prognosis, including age, AJCC stage, ISUP grade, and the 6-IRL signature, to develop a practical clinical prediction tool aimed at enhancing the accuracy of survival predictions for ccRCC patients. This predictive model, represented by a nomogram, estimates the 1-year, 3-year, and 5-year survival probabilities of ccRCC patients (Fig. 8A). To further validate the accuracy of the Nomogram model, we constructed calibration curves (Fig. 8B). The calibration curves compare the predicted survival rates with the actual observed survival rates. The results show that the Nomogram performs well in predicting survival, with predicted values closely aligning with actual survival outcomes. The calibration curve is close to the diagonal, indicating high predictive accuracy. Additionally, we employed decision curve analysis (DCA) to further assess the clinical utility of the tool. The DCA results indicated that the nomogram provided greater net benefits and a wider range of threshold probabilities in predicting 1-year, 3-year, and 5-year survival. Compared to the 6-IRL signature alone, the nomogram exhibited superior clinical applicability (Fig. 8C–F).

Immune analysis via 6-IRLs markers

According to the results of Gene Set Enrichment Analysis (GSEA), we observed significant enrichment differences in multiple KEGG pathways between the high-risk and low-risk groups (Fig. 9A). In the high-risk group, the T-cell receptor (TCR) signaling pathway and Toll-like receptor (TLR) signaling pathway exhibited positive enrichment scores, suggesting that cells in the high-risk group may rely on enhanced innate immune receptor signaling to cope with greater metabolic and inflammatory stress. Conversely, the glutathione metabolism pathway, fatty acid metabolism, and TGF-β signaling pathway were significantly enriched in the low-risk group, implying that cells in this group might shift towards fatty acid oxidation metabolism, accompanied by augmented TGF-β

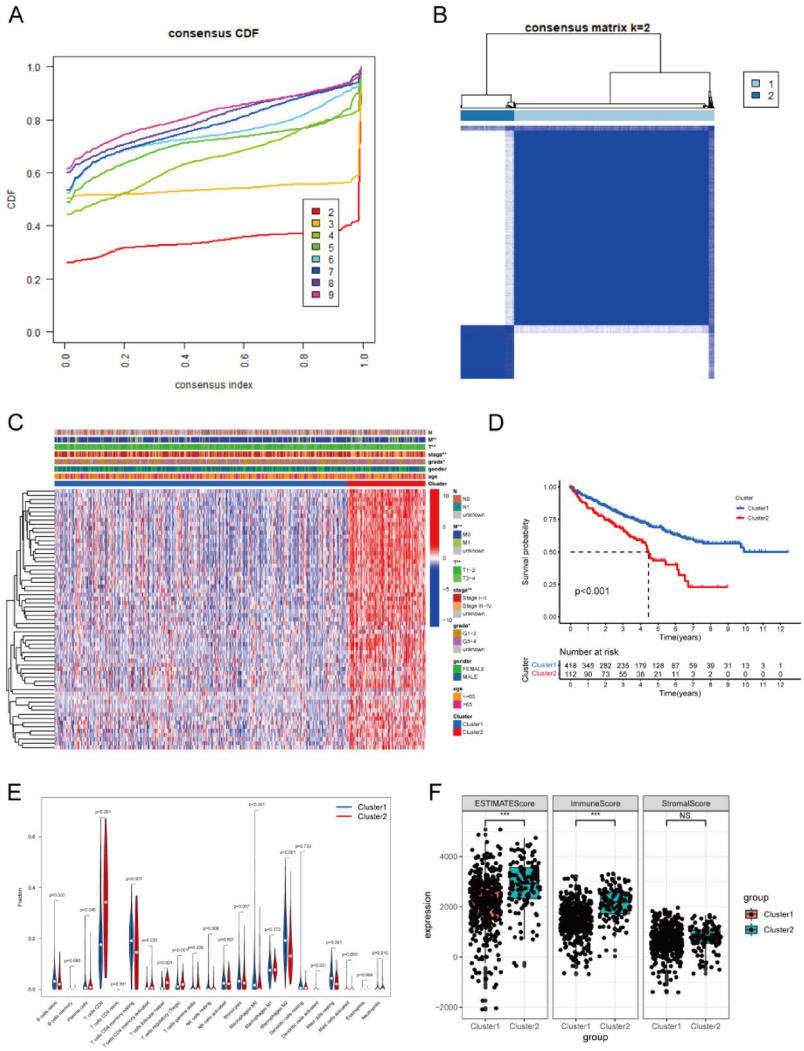

Fig. 4. Cluster analysis of the TCGA-KIRC dataset using key IRLs. (**A**, **B**) The consistency clustering results indicate that ccRCC patients can be effectively divided into two clusters; (**C**) Heatmaps and associated clinical-pathological features in two clusters; (**D**) Survival curves for the two clusters; (**E**) Different immune cell infiltrations between the two clusters; (**F**) Differences in tumor microenvironment scores between the two clusters. (*,$P<0.05$;**,$P<0.01$; ***,$P<0.001$). IRLs, IL2RG -related lncRNAs; CDF, cumulative distribution function.

signaling, which was suppressed in the high-risk group. This enrichment could indicate that cells in the low-risk group maintain metabolic homeostasis and altered immune suppression signals, making them less prone to severe disease progression, a capacity lacking in the high-risk group. Furthermore, the P53 signaling pathway and autophagy regulation also showed differential enrichment across the risk spectrum, hinting at a complex regulatory network involving tumor suppression and autophagic processes that may influence the phenotypic transition between high-and low-risk groups.

Subsequently, we delved deeper into the enrichment levels and activities of immune cells, relevant pathways, and their functions in ccRCC. The results revealed significant differences in immune marker expression between the low-risk and high-risk groups (Fig. 9B). Further analysis of immune checkpoint expression between the two groups indicated substantial differences across several immune checkpoint molecules (Fig. 9C). Additionally, we evaluated the correlation between risk scores and immune cell infiltration. The analysis showed a positive correlation between risk scores and Memory B cells, Neutrophils, M1 macrophages, CD8 + T cells, Regulatory T cells, and Follicular helper T cells. In contrast, M2 macrophages, resting Mast cells, naive B cells, Monocytes, Eosinophils, activated Dendritic cells, and resting Dendritic cells were negatively correlated with risk scores (Fig. 9D–G, Fig. S8).

To further investigate the cellular localization of the 6-IRLs within the TME, we utilized the Tumor Immune Single-cell Hub 2 (TISCH2) database, which provides curated single-cell RNA sequencing data with annotated immune and stromal cell types. Five ccRCC-related datasets (GSE111360, GSE139555, GSE121636, GSE159115, and GSE171306) were analyzed. The results showed that multiple IRLs within the signature were predominantly

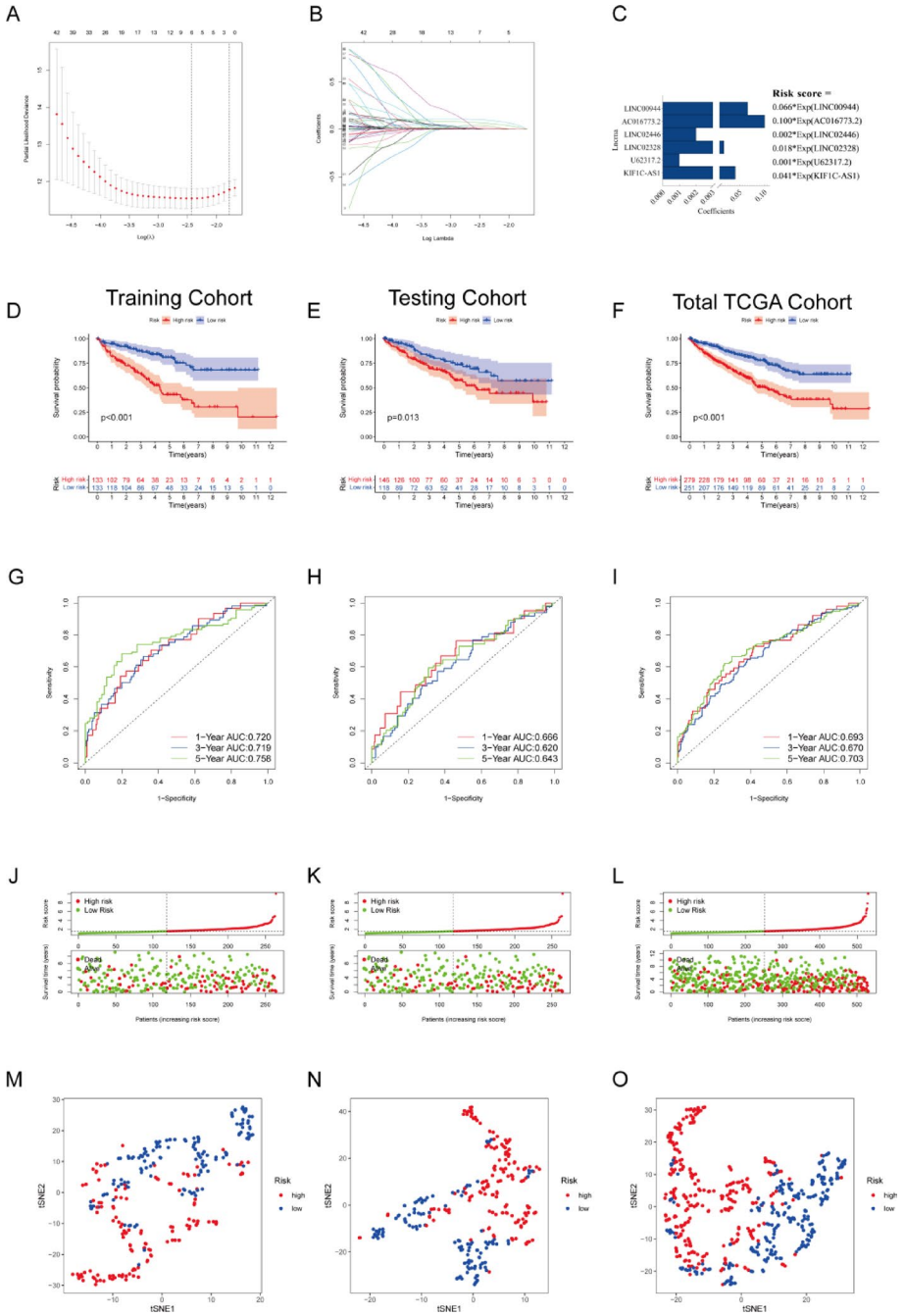

Fig. 5. (**A**–**C**) Construction of the 6-IRLs model using LASSO regression and risk scoring formula; (**D**–**F**) Overall survival (OS) of high- and low-risk score groups in the training, testing, and TCGA cohorts; (**G**–**I**) ROC curves for high- and low-risk score groups in the training, testing, and TCGA cohorts; (**J**–**L**) Survival status curves and scatter plots for high- and low-risk score groups in the training, testing, and TCGA cohorts; (**M**–**O**) t-SNE distribution of high- and low-risk score groups in the training, testing, and TCGA cohorts. (*$P<0.05$; **$P<0.01$; ***$P<0.001$). LASSO: Least Absolute Shrinkage and Selection Operator; ROC: Receiver Operating Characteristic; t-SNE: t-distributed Stochastic Neighbor Embedding.

enriched in immune effector populations, particularly $CD4^+$ T cells, $CD8^+$ T cells, and NK cells (Fig. S9), indicating their potential immune-related distribution patterns in the ccRCC microenvironment.

Drug sensitivity analysis

In our study, we focused on five commonly used targeted drugs in clinical practice: Sunitinib, Temsirolimus, Sorafenib, Pazopanib, and Axitinib. These drugs were selected due to their frequent use in the treatment of advanced ccRCC and other cancers.

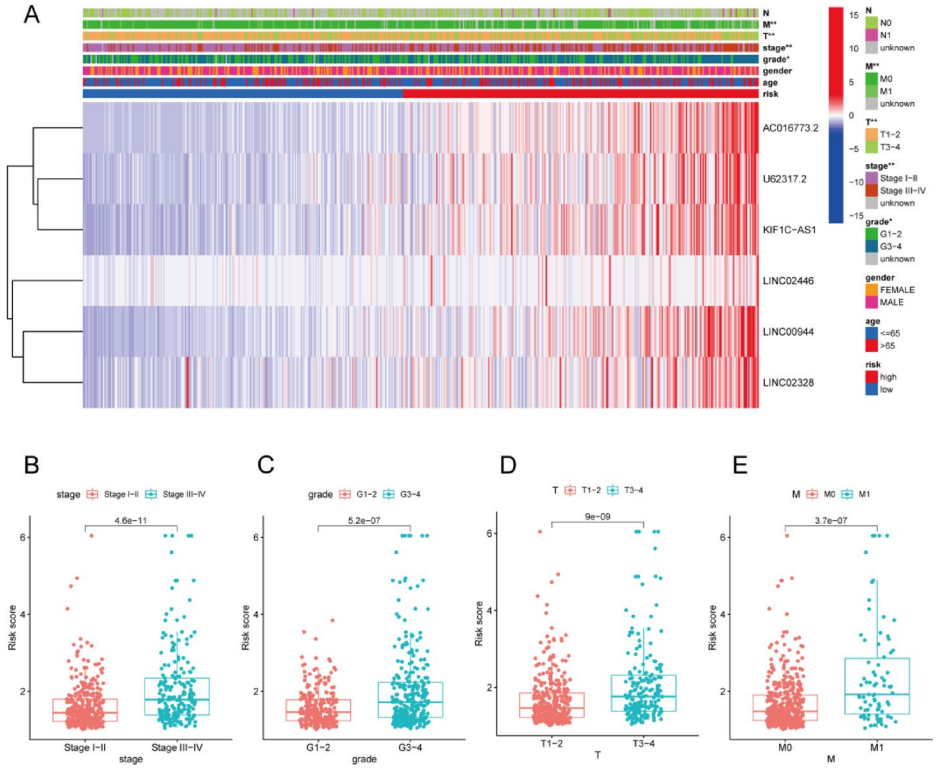

Fig. 6. Correlation between the 6-IRLs model and clinical pathological features. (**A**) The heatmap between the 6-IRLs model and clinical pathological features; (**B**–**E**) Clinical correlation analysis of high-and low-risk scores with patients (*,$P<0.05$;**,$P<0.01$).

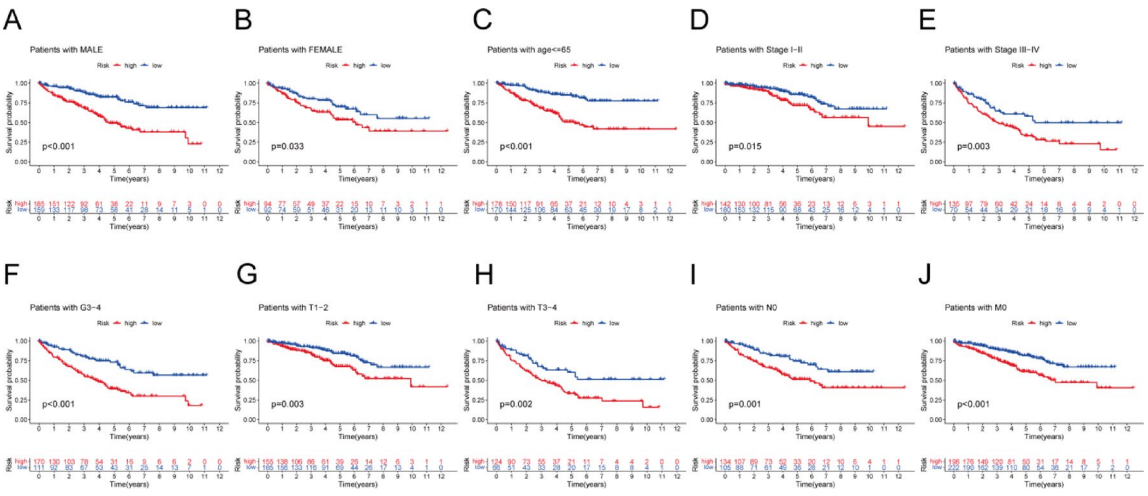

Fig. 7. Stratified prognostic value of the 6-IRLs signature. OS differences between the high-risk and low-risk groups based on gender (**A**, **B**), age (**C**), stage (**D**, **E**), grade (**F**), T stage (**G**, **H**), N0 stage (**I**), and M0 stage (**J**).

The sensitivity analysis of commonly used targeted drugs revealed that the high-risk group exhibited greater sensitivity to Sunitinib and Temsirolimus (Fig. 10A, C), while the low-risk group demonstrated higher sensitivity to Sorafenib and Pazopanib (Fig. 10B, E). Conversely, Axitinib showed no significant difference between the two groups ($p=0.55$) (Fig. 10D). It is possible that the lack of a significant difference is due to the multifaceted mechanism of action of Axitinib, which depends on the complex interplay of various factors, including the tumor immune microenvironment. Specifically, the high-risk group may have an immune-suppressive microenvironment (e.g., regulatory T cells), which could potentially diminish the effectiveness of Axitinib, whereas the immune environment in the low-risk group may be more conducive to its action. This result highlights the complexity of drug sensitivity.

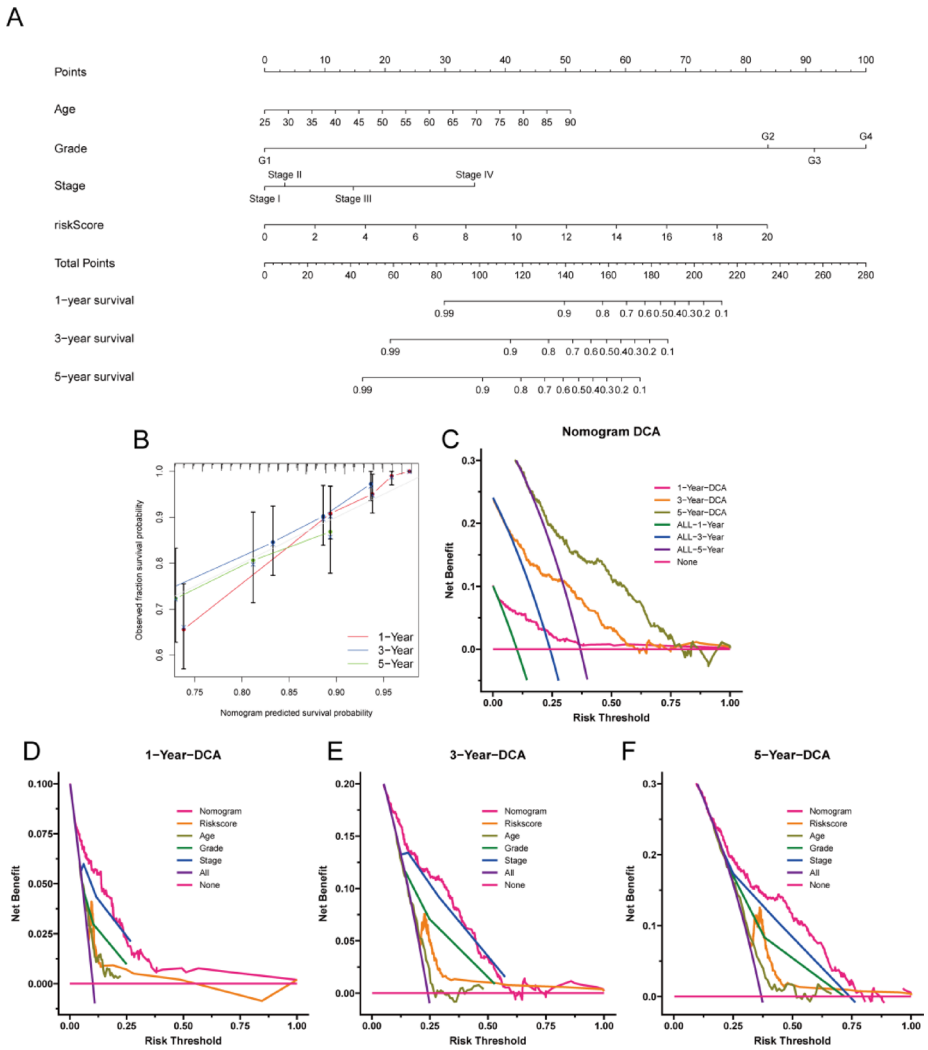

Fig. 8. The establishment and validation of the nomogram based on 6-IRLs. (**A**) Prognostic nomogram based on the 6-IRLs signature and clinical pathological parameters; (**B**) Calibration curves for 1-year, 3-year, and 5-year nomograms; (**C**–**F**) DCA analysis shows the clinical benefits of the nomogram at 1 year, 3 years, and 5 years. DCA, Decision Curve Analysis.

These results suggest a correlation between risk group stratification and drug sensitivity. Furthermore, the 6-IRLs signature could serve as an independent predictor of drug efficacy, potentially holding significant clinical value.

Clinical sample validation

QRT-PCR was used to evaluate the -lncRNAs expression levels in 50 paired sets of ccRCC tissues and the adjacent normal tissues. Tissue sections of pathological origin were obtained from patients with confirmed ccRCC through pathological assessment.The results indicated that the relative expression levels of 6-lncRNAs were significantly elevated in ccRCC tumor tissues compared to adjacent normal tissues, with all differences being statistically significant (Fig. 11A–F) ($P < 0.05$). These experimental findings corroborate our bioinformatics analysis, reaffirming the accuracy of our study through the confirmed expression levels of the 6-lncRNAs.

Discussion

Renal cell carcinoma (RCC), commonly referred to as kidney cancer, comprises a group of heterogeneous epithelial tumors with malignant characteristics, with clear cell carcinoma being the predominant subtype, accounting for approximately 80%[36]. Given that ccRCC often presents with subtle early clinical symptoms, it is frequently diagnosed only after metastasis has occurred, with a five-year overall survival rate for metastatic RCC patients falling below 10%[37]. Consequently, it is crucial to explore new diagnostic approaches for ccRCC patients and to enhance overall survival rates. The intricate interactions between tumor cells and immune components within the tumor microenvironment (TME) shape the tumor's immune response, which can both promote and inhibit tumor growth[38]. Therefore, investigating immune-related factors within the TME is of significant importance for developing effective cancer immunotherapies.

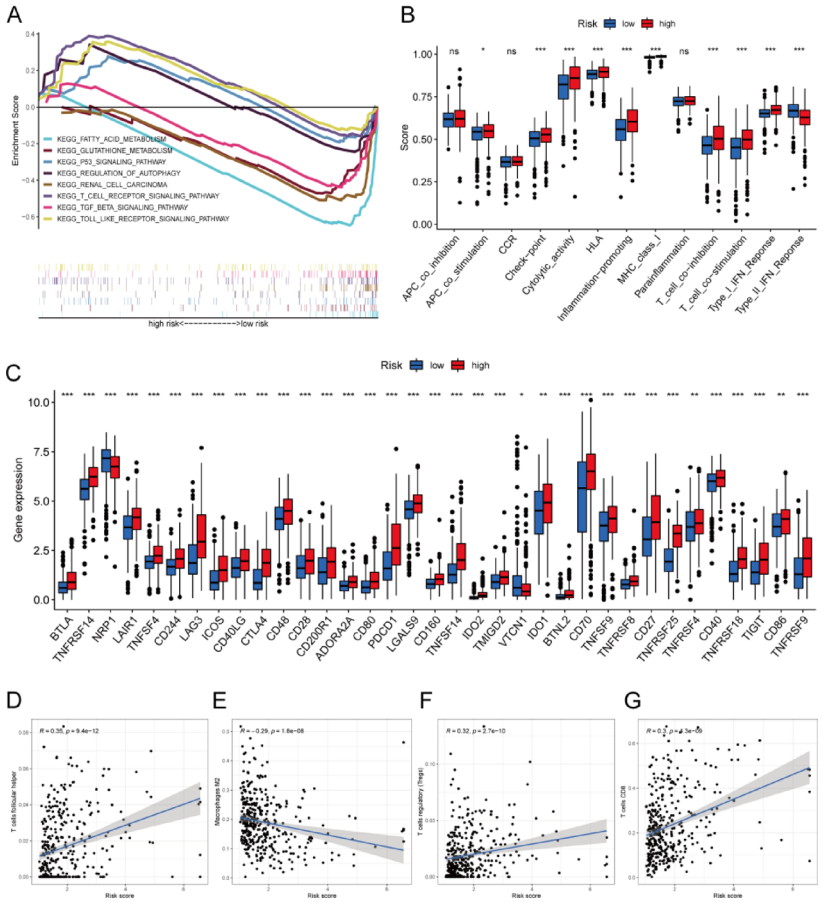

Fig. 9. Functional enrichment analysis based on high-risk or low-risk groups. (**A**) GSEA enrichment analysis; (**B**) Immune function analysis based on high-risk or low-risk group; (**C**) Expression of immune checkpoints analysis based on high-risk or low-risk group; (**D**–**G**) Correlation analysis between risk scores and immune cell infiltration.(*,$P<0.05$;**,$P<0.01$; ***,$P<0.001$). GSEA, Gene Set Enrichment Analysis.

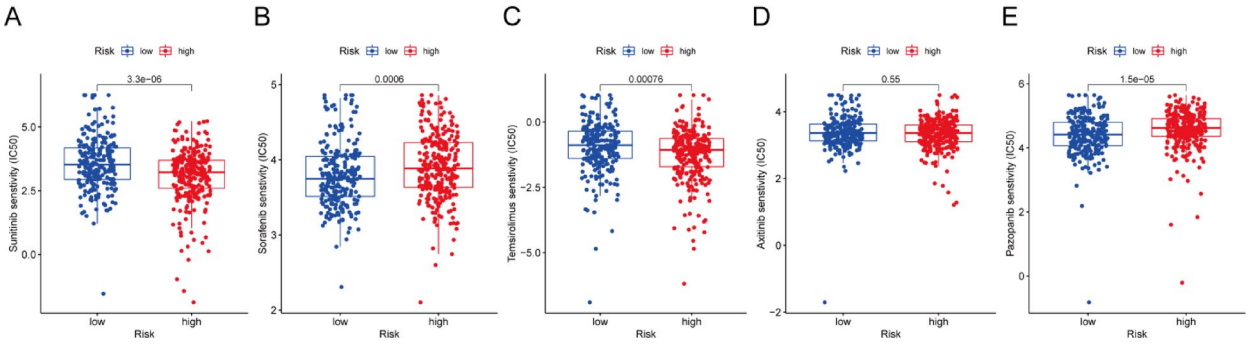

Fig. 10. Drug sensitivity analysis. Differences in drug sensitivity between high-risk and low-risk groups for Sunitinib (**A**), Sorafenib (**B**), Temsirolimus (**C**), Axitinib (**D**), and Pazopanib (**E**).

IL2RG is a single-pass transmembrane protein, with its intracellular segments responsible for activating downstream signaling pathways, particularly the JAK/STAT pathway, which plays a pivotal role in immune regulation[39]. In recent years, the role of IL2RG in tumor immune modulation has been increasingly elucidated. IL2RG mediates the signaling of IL-2 and other cytokines, playing a crucial role in the activation and function of immune cells within the tumor microenvironment[40]. The interaction between IL-2 and IL2RG enhances the cytotoxicity of T cells and NK cells, promoting their ability to target and kill tumor cells[41]. However, in melanoma, tumor cells employ various mechanisms to suppress IL2RG-related signaling pathways, leading to immune evasion and subsequently promoting tumor growth and metastasis[42]. lncRNAs play a significant regulatory role in tumor initiation and progression[20,21]. As biomarkers, they are becoming increasingly important in clinical

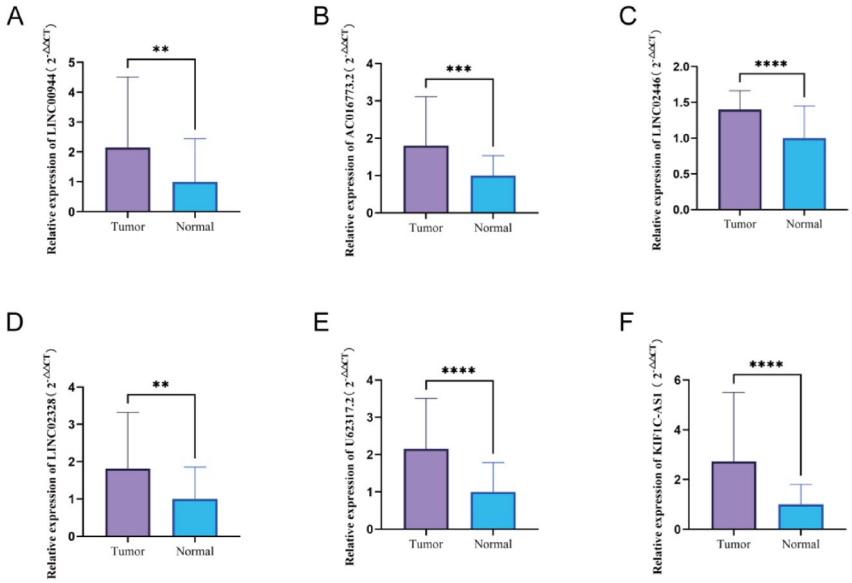

Fig. 11. Tissue validation of 6-IRLs expression. (**A**) qRT-PCR assessment of LINC00944 (**A**), AC016773.2 (**B**), LINC02446 (**C**), LINC02328 (**D**), U62317.2 (**E**), KIF1C-AS1 (**F**) expression in ccRCC tissues compared to normal tissues ($n = 50$). (*,$P < 0.05$;**,$P < 0.01$;***,$P < 0.001$).

treatment, yet there is limited reporting on IRLs related to ccRCC prognosis. Therefore, constructing a prognosis model based on IRLs from the TCGA database and exploring new biomarkers and therapies holds significant promise for the treatment of ccRCC.

In this study, we thoroughly investigated the role of IL2RG in ccRCC and its potential as a prognostic biomarker. Pan-cancer analysis revealed dysregulation of IL2RG across various cancers, suggesting its involvement in tumorigenesis through diverse mechanisms. Specifically, in ccRCC tissues and cells, qRT-PCR and IHC assays demonstrated a significant upregulation of IL2RG expression compared to normal tissues, underscoring its crucial role in ccRCC progression. Furthermore, IL2RG expression levels were closely associated with tumor progression, including T staging, N staging, M staging, and patient prognosis. This suggests that IL2RG may play a pivotal role in the onset, development, and prognosis of ccRCC. Subsequent research on immune-related genes revealed significant correlations between IL2RG and several immune genes, particularly highlighting the dysregulation of 26 key immune-related genes in ccRCC. This emphasizes the intricate interplay between IL2RG and the tumor immune microenvironment. After performing consistent clustering of ccRCC patients using 63 key IRLs, we found that grouping patients into two clusters based on these IRLs was feasible. 63 IRLs are associated with patient prognosis, further supporting the potential of these immune-related genes as therapeutic targets.

By identifying 63 key IRLs and utilizing LASSO regression analysis to construct a prognostic model based on 6-IRLs (LINC00944, AC016773.2, LINC02446, LINC02328, U62317.2, KIF1C-AS1), the pivotal role of lncRNAs in ccRCC has been underscored. They are involved in regulating IL2RG expression and modulating the TME.LINC00944, for instance, may interact with miRNAs to regulate IL2RG, influencing immune responses and potentially promoting immune evasion in ccRCC[43]. Although the direct interaction between the lncRNA and IL2RG has not been fully elucidated, they may indirectly regulate IL2RG via upstream signaling pathways, such as the JAK/STAT pathway and the NF-κB pathway, which are involved in immune cell activation and cytokine secretion[44]. LINC00944 and other immune-related lncRNAs may also contribute to shaping the immunosuppressive microenvironment by modulating the expression of immune checkpoint molecules (e.g., PD-L1) or regulating the secretion of pro-inflammatory cytokines[45]. For instance, LINC00944 might alter the balance between immune activation and suppression by influencing the infiltration of CD8 + T cells or Tregs. By affecting cytokine secretion, such as IL-2 and TNF-α, these lncRNAs could impair tumor immune surveillance, thereby promoting immune evasion and metastasis[46].while Chen et al. experimentally showed that knocking down LINC00944 significantly reduces proliferation and migration, and enhances Akt phosphorylation[47]. Furthermore, Pamela's sequencing work revealed that LINC00944 might be associated with tumor-infiltrating T lymphocytes and apoptotic pathways in breast cancer[48]. Similarly, AC016773.2 and LINC02446 might regulate immune cell infiltration and function, contributing to the formation of an immunosuppressive TME. Liu et al. found that AC016773.2 could be related to m6A methylation[45]. Wu et al. identified that LINC02446 is linked to epithelial-mesenchymal transition (EMT) in bladder cancer[49]and Zhang et al. demonstrated that LINC02446 regulates the mTOR signaling pathway by binding to EIF3G, thereby inhibiting bladder cancer cell proliferation and metastasis, and potentially correlates with ferroptosis[50,51]. LINC02328 may be associated with endoplasmic reticulum stress in osteosarcoma, while U62317.2 has been confirmed to be potentially related to EMT in bladder cancer, and may also be involved in regulating interferon response and RNA surveillance through nonsense-mediated decay (NMD)[52,53].

Taken together, these findings suggest that the 6-IRLs incorporated into the prognostic model may participate in a coordinated regulatory network affecting tumor progression and immune modulation in ccRCC. Several of these lncRNAs, such as LINC00944, LINC02328, and U62317.2, appear to engage in immune-related signaling, including the regulation of cytokine secretion, immune checkpoint molecules, and immune cell infiltration—all of which are closely tied to the function of IL2RG. Moreover, their involvement in canonical immune-related pathways, such as JAK/STAT and NF-κB signaling, further implies a potential convergence on IL2RG-mediated immune regulation. Consistent with their predicted functional roles, our experimental validation demonstrated that these six IRLs exhibit significantly dysregulated expression in ccRCC tissues compared to adjacent normal tissues, supporting their relevance in tumor biology. While direct mechanistic links remain to be fully elucidated, these IRLs may act through ceRNA interactions or epigenetic mechanisms to influence IL2RG expression and downstream immune activity. This integrative role highlights their potential as both prognostic markers and modulators of the immunosuppressive tumor microenvironment. Understanding the precise mechanisms by which these lncRNAs regulate IL2RG and the TME will provide valuable insights into cancer immunology and offer potential therapeutic targets for immune modulation.

Subsequently, this prognostic model was validated in both the testing cohort and the TCGA cohort, with the scoring formula serving as a reliable prognostic indicator. Analysis of various clinical parameters in relation to the 6-IRLs signature revealed significant differences between high- and low-risk groups, underscoring its clinical predictive value. The 6-IRLs signature was found to be closely associated with overall survival (OS). We constructed a nomogram for risk scoring, predicting the 1-, 3-, and 5-year survival rates of ccRCC patients, with calibration and decision curve analyses confirming its high accuracy and sensitivity.Although our model demonstrated robust prognostic performance within the TCGA-KIRC cohort through internal validation, we also sought to assess its generalizability in an independent external dataset. However, due to the limited coverage of lncRNA expression in public datasets, only four of the 6 IRLs (LINC00944,LINC02446,LINC02328,KIF1C-AS1) were available in the GSE167573 cohort. Despite this limitation, we applied a 4-IRLs–based model and observed a trend toward worse overall survival in the high-risk group, though the difference did not reach statistical significance ($P = 0.065$), likely due to the small sample size ($n = 54$) and broad confidence intervals.While the findings from this external validation are preliminary, they suggest the potential of the model to stratify patients beyond the training dataset. More importantly, this highlights a broader challenge in the field—namely, the lack of high-quality, lncRNA-complete and clinically annotated ccRCC cohorts suitable for independent validation of lncRNA-based models.

Although the proposed 6-IRLs model demonstrated promising survival prediction capabilities, we further assessed its clinical utility by comparing it with widely used prognostic tools. Specifically, we compared it with the traditional TNM staging system. The results indicated that the 6-IRLs model showed superior prognostic accuracy in survival prediction, providing a more refined risk stratification compared to TNM staging, as evidenced by Cox regression analysis and Kaplan-Meier survival curves.

Moreover, although existing lncRNA-based prognostic models have shown some predictive value, they often face limitations in differentiating ccRCC subtypes or molecular characteristics. In contrast, our 6-IRLs model integrates the expression profiles of multiple lncRNAs, offering a more personalized prognostic assessment for ccRCC patients. Therefore, our findings suggest that the 6-IRLs model could serve as a valuable supplementary tool, potentially enhancing the accuracy of clinical diagnosis and therapeutic decision-making when combined with traditional TNM staging.

Exploration of TME-related pathways through GSEA revealed distinct enrichment patterns between the high- and low-risk groups, with high-risk patients exhibiting increased activity in innate immune pathways, while low-risk patients displayed a greater tendency towards metabolic homeostasis. This suggests that targeted therapies focusing on specific metabolic or immune pathways may provide therapeutic benefits for the distinct ccRCC subtypes defined by the risk score groups. The immune-related findings of this study also highlight the profound impact of IRLs on the immune landscape of ccRCC. Consensus clustering based on IRL expression uncovered two distinct subtypes of ccRCC, each characterized by unique immune cell infiltration patterns. Differential infiltration of CD8 + T cells, M1 and M2 macrophages, B cells, and regulatory T cells between the groups indicates that the immune response within the TME is intricately linked to the expression of these lncRNAs. These immune cell types play crucial roles in both tumor suppression and immune evasion.

Interestingly, our study revealed that the TME of high-risk patients is characterized by an increase in immunosuppressive cells, such as regulatory T cells, which are often associated with poor prognosis and resistance to immunotherapy[54]. The enrichment of TLRs and TCRs signaling pathways in the high-risk group suggests that these patients may exhibit an active but dysregulated immune system. The heightened presence of TLRs signaling could reflect a stronger inflammatory response[55]while the aberrant activation of TCRs signaling implies that effector T cells might be in a state of functional exhaustion[56]. This indicates that the TME in high-risk patients may favor tumor progression rather than an effective anti-tumor immune response. These findings underscore the pivotal role of immune pathways in high-risk patients and offer a new direction for future research aimed at improving prognosis through targeted immunotherapies.

In contrast, the enrichment of glutathione metabolism and TGF-β signaling pathways in the low-risk group suggests stronger antioxidant and immunosuppressive capabilities[57,58]. This may indicate that the TME in low-risk patients is in a more quiescent immune state, with reduced oxidative stress and inflammatory responses, allowing the immune system to better maintain tissue homeostasis. Enhanced glutathione metabolism helps mitigate oxidative damage, while active TGF-β signaling points to strengthened immunosuppressive and tissue repair mechanisms[57,58]. Collectively, the enrichment of these pathways may contribute to preventing tumor progression and lead to a more favorable prognosis in ccRCC.

Analysis of the immune microenvironment in ccRCC revealed significant differences in immune cell infiltration patterns between the low and high-risk groups, which may influence clinical outcomes and

therapeutic responses. Further analysis of immune checkpoint expression further highlighted the differences in immune microenvironment between the two groups. Specifically, the high-risk group exhibited elevated expression of immune checkpoints, suggesting an immunosuppressive state in the tumor microenvironment that may promote immune evasion.

We also assessed the correlation between risk scores and immune cell infiltration, which provided valuable insights into the immune cell composition across different risk groups. Notably, we found a positive correlation between risk scores and multiple immune cell populations, including memory B cells, neutrophils, M1 macrophages, CD8 + T cells, regulatory T cells (Tregs), and follicular helper T cells. These immune cells often play dual roles in both anti-tumor immunity and immune suppression[59]suggesting the presence of such dual roles in the progression of ccRCC. For instance, while CD8 + T cells and M1 macrophages are typically associated with anti-tumor responses[60]their presence in the high-risk group might indicate an ongoing immune response in the tumor microenvironment, which could be suppressed or regulated by other factors.

On the other hand, the risk score negatively correlated with certain immune cell types (e.g., M2 macrophages, resting mast cells, naïve B cells, monocytes, eosinophils, activated dendritic cells, and resting dendritic cells), suggesting altered immune dynamics in the high-risk group. In particular, M2 macrophages, widely recognized for their role in promoting tumor progression, immune suppression, and tissue remodeling, were reduced or functionally impaired in the high-risk group[61]. This may reflect a mechanism of tumor escape from immune surveillance, often associated with poor prognosis and treatment resistance.

The immune microenvironment in the high-risk group revealed concerns regarding treatment resistance, particularly in immunotherapy. High expression of immune checkpoint molecules and skewed immune cell composition may diminish the effectiveness of immune checkpoint inhibitors by creating an immunosuppressive tumor microenvironment[62]. For example, the increased presence of Tregs is closely related to immune suppressive responses, which may limit the activation of the immune system, thus reducing the efficacy of immunotherapy[63]. Moreover, the reduced presence of activated dendritic cells and eosinophils in the high-risk group suggests that the tumor may evade immune attack by suppressing the activation pathways of these cells, further supporting the link between immune evasion and treatment resistance[64].These immune features may also help explain the clinical phenomenon of treatment resistance in ccRCC patients undergoing immunotherapy or other targeted therapies.

Therefore, future studies should further explore strategies to modulate these immune cell populations to enhance treatment responses. Specifically, targeted approaches aimed at immune evasion mechanisms, particularly by reducing the role of immunosuppressive cells (such as M2 macrophages and Tregs) or enhancing the activity of pro-inflammatory immune cells (such as CD8 + T cells and M1 macrophages), could significantly improve clinical outcomes in high-risk patients.

Subsequently, our research revealed that IRLs play a crucial role in guiding clinical treatment for cancer patients. We identified a significant correlation between the IRL gene risk model and drug sensitivity.

In our study, we focused on five commonly used targeted drugs in clinical practice: Sunitinib, Temsirolimus, Sorafenib, Pazopanib, and Axitinib. These drugs were selected because they are frequently employed in the treatment of advanced ccRCC and other cancers[5]. Sunitinib, for example, is widely used in the first-line treatment of metastatic ccRCC due to its anti-angiogenic effects through inhibition of VEGF receptors[65]. Temsirolimus, an mTOR inhibitor, is often applied to patients with poor prognosis or in advanced stages of ccRCC, particularly when resistance to other therapies is observed[66]. Sorafenib and Pazopanib are multi-targeted kinase inhibitors that have been shown to be effective in ccRCC treatment, particularly in advanced stages and when there is metastasis[67]. Axitinib, another VEGF receptor inhibitor, is often considered for patients who have progressed after first-line treatments like Sunitinib or Sorafenib[68].

Our findings revealed that high-risk patients demonstrated heightened sensitivity to Sunitinib and Temsirolimus, whereas low-risk individuals responded more favorably to Sorafenib and Pazopanib. Although all four agents exert anti-angiogenic effects—either directly or indirectly—through inhibition of VEGF receptors, they differ substantially in their target spectra[69–72]signaling pathway modulation, and pharmacodynamic profiles, which may underlie the observed heterogeneity in therapeutic responses across risk groups.

Specifically, both Sunitinib and Temsirolimus act not only on VEGFR but also converge on the mTOR pathway—a critical signaling axis implicated in immune suppression, tumor angiogenesis, and metabolic reprogramming in highly aggressive malignancies.High-risk individuals may exhibit a greater dependence on this VEGF/mTOR-driven circuitry, rendering them more susceptible to agents that co-target these axes[70,72,73]. In contrast, Sorafenib and Pazopanib, while also targeting VEGFR, possess broader kinase inhibition profiles encompassing the RAF/MEK/ERK cascade, c-KIT, PDGFR, and other metabolism-associated molecules[74,75]. In the low-risk group, pathway enrichment analysis revealed upregulation of multiple metabolic programs—particularly those related to fatty acid metabolism—accompanied by a marked suppression of pro-inflammatory signaling, which may establish a tumor microenvironment more amenable to multi-targeted kinase inhibition. These findings suggest that IRLs may modulate drug responsiveness by orchestrating immune-metabolic states and pathway dependencies in a risk-dependent manner.

Collectively, these results highlight that despite overlapping mechanisms of action, the clinical efficacy of targeted therapies can be profoundly shaped by the underlying molecular landscape, signaling dynamics, and IRL-mediated regulatory networks.From a translational perspective, the 6-IRL–based risk signature offers a clinically actionable stratification tool that not only predicts prognosis but also informs therapeutic decision-making.For instance, patients classified as high-risk who may exhibit greater reliance on VEGF/mTOR signaling—might derive more benefit from Sunitinib or Temsirolimus, whereas low-risk patients with metabolic enrichment and attenuated inflammatory signaling may respond better to Sorafenib or Pazopanib.This risk-adapted treatment paradigm holds promise for improving therapeutic precision, minimizing unnecessary toxicity, and ultimately enhancing survival outcomes in ccRCC.

Overall, the 6-IRLs signature offers a promising tool for enhancing personalized treatment strategies in ccRCC, guiding clinicians in selecting the most appropriate targeted therapies based on an individual patient's risk profile and predicted drug sensitivity. This approach could improve treatment efficacy, reduce adverse effects, and ultimately improve patient survival outcomes.

In addition, Compared the prognostic performance of the 6-IRLs with six previously published representative prognostic models for ccRCC: immune-related gene signatures[76]EMT-related lncRNA signatures[77]machine learning-based ceRNA network models[78]immune-related lncRNA pair signatures[79]a four-lncRNA panel validated in an external cohort[80]and immune gene-based predictors of immunotherapy response[81],our 6-IRLs model demonstrated superior or comparable performance in multiple survival indicators, including AUC and C-index, and remained an independent prognostic factor in multivariate analyses.

Notably, our model was constructed based on IL2RG, a pivotal immune regulatory gene implicated in multiple cytokine signaling pathways and T-cell homeostasis. The six IRLs included in the model were systematically identified as IL2RG-related and immune-associated lncRNAs, reflecting their potential roles in shaping the tumor immune microenvironment. This mechanistically grounded approach distinguishes our model from other lncRNA-based signatures that rely on statistical selection alone. Furthermore, the concise structure of the 6-IRLs model enhances its interpretability and clinical feasibility, offering a biologically informed and practically valuable tool for prognostic stratification and immunotherapy decision-making in ccRCC.

In conclusion, the 6-ILRs signature developed in this study provides a powerful tool for risk stratification and treatment decision-making in ccRCC, highlighting the critical role of the 6-ILRs in shaping the immune landscape, influencing patient prognosis, and determining treatment outcomes. The immune microenvironment analysis based on the 6-ILRs signature not only offers more accurate prognostic assessments for ccRCC patients but may also become a key tool for personalized immunotherapy. By further investigating the role of these immune-related lncRNAs in immune evasion mechanisms, the 6-ILRs signature holds promise in providing new insights for the development of immunotherapy targets, ultimately advancing the realization of precision treatment.

However, the clinical utility of this model requires further validation in larger, independent cohorts. Additionally, mechanistic studies are needed to elucidate the precise roles of these lncRNAs in regulating immune responses and influencing drug sensitivity. Integrating multi-omics data, including epigenomics and proteomics, may offer deeper insights into how these lncRNAs orchestrate complex tumor-immune interactions.

Conclusions

This study elucidates the expression profile of IL2RG in ccRCC and its potential role as a prognostic marker, validated through qRT-PCR and IHC. Based on the expression characteristics of IL2RG and its immune-related genes, we identified and constructed a 6-IRLs signature model. The findings demonstrate that this model can serve as an effective tool for diagnosing and predicting the prognosis of renal cell carcinoma patients. This research offers new insights into the regulatory mechanisms of renal cell carcinoma and provides a novel reference framework for the development of clinical immunotherapies and personalized targeted treatment strategies.

Data availability

The datasets generated during and/or analysed during the current study are available from the corresponding author on reasonable request.

Received: 4 February 2025; Accepted: 7 August 2025
Published online: 13 August 2025

References

1. Kim, H. et al. Loss of von Hippel-Lindau (VHL) tumor suppressor gene function: VHL-HIF pathway and advances in treatments for metastatic renal cell carcinoma (RCC). *Int. J. Mol. Sci.* **22** https://doi.org/10.3390/ijms22189795 (2021).
2. Sung, H. et al. Global cancer statistics 2020: GLOBOCAN estimates of incidence and mortality worldwide for 36 cancers in 185 countries. *CA Cancer J. Clin.* **71**, 209–249. https://doi.org/10.3322/caac.21660 (2021).
3. Jonasch, E., Walker, C. L. & Rathmell, W. K. Clear cell renal cell carcinoma ontogeny and mechanisms of lethality. *Nat. Rev. Nephrol.* **17**, 245–261. https://doi.org/10.1038/s41581-020-00359-2 (2021).
4. Qian, C. N. Hijacking the vasculature in ccRCC–co-option, remodelling and angiogenesis. *Nat. Rev. Urol.* **10**, 300–304. https://doi.org/10.1038/nrurol.2013.26 (2013).
5. Hsieh, J. J. et al. Renal cell carcinoma. *Nat. Rev. Dis. Primers*. **3**, 17009. https://doi.org/10.1038/nrdp.2017.9 (2017).
6. Huang, Y., Sun, H. & Guo, P. Research progress of tumor microenvironment targeted therapy for clear cell renal cell carcinoma. *Cancer Control.* **30**, 10732748231155700. https://doi.org/10.1177/10732748231155700 (2023).
7. Lin, J. X. & Leonard, W. J. The common cytokine receptor γ chain family of cytokines. *Cold Spring Harb Perspect. Biol.* **10** https://doi.org/10.1101/cshperspect.a028449 (2018).
8. Winer, H. et al. IL-7: comprehensive review. *Cytokine* **160**, 156049. https://doi.org/10.1016/j.cyto.2022.156049 (2022).
9. Cavazzana, M., Six, E., Lagresle-Peyrou, C., André-Schmutz, I. & Hacein-Bey-Abina, S. Gene therapy for X-Linked severe combined immunodeficiency: where do we stand? *Hum. Gene Ther.* **27**, 108–116. https://doi.org/10.1089/hum.2015.137 (2016).
10. Baldasici, O. et al. The transcriptional landscape of cancer stem-like cell functionality in breast cancer. *J. Transl Med.* **22**, 530. https://doi.org/10.1186/s12967-024-05281-w (2024).
11. Bilotta, M. T., Antignani, A. & Fitzgerald, D. J. Managing the TME to improve the efficacy of cancer therapy. *Front. Immunol.* **13**, 954992. https://doi.org/10.3389/fimmu.2022.954992 (2022).
12. Lasorsa, F. et al. Cellular and molecular players in the tumor microenvironment of renal cell carcinoma. *J. Clin. Med.* **12** https://doi.org/10.3390/jcm12123888 (2023).
13. Donnenberg, V. S., Huber, A., Basse, P., Rubin, J. P. & Donnenberg, A. D. Neither epithelial nor mesenchymal circulating tumor cells isolated from breast cancer patients are tumorigenic in NOD-scid Il2rg(null) mice. *NPJ Breast Cancer*. **2**, 16004. https://doi.org/10.1038/npjbcancer.2016.4 (2016).

14. Melsen, J. E. et al. T and NK cells in IL2RG-Deficient patient 50 years after hematopoietic stem cell transplantation. *J. Clin. Immunol.* **42**, 1205–1222. https://doi.org/10.1007/s10875-022-01279-5 (2022).
15. Ranson, T. et al. IL-15 is an essential mediator of peripheral NK-cell homeostasis. *Blood* **101**, 4887–4893. https://doi.org/10.1182/blood-2002-11-3392 (2003).
16. Zheng, Y., Liu, J., Li, Y. & Huang, J. IL-2RG is a predictor of prognosis and response to immune checkpoint blockages and is correlated with immune infiltrates in breast cancer. *Asian J. Surg.* **46**, 5359–5361. https://doi.org/10.1016/j.asjsur.2023.07.114 (2023).
17. Bridges, M. C., Daulagala, A. C. & Kourtidis, A. LNCcation: LncRNA localization and function. *J. Cell. Biol.* **220** https://doi.org/10.1083/jcb.202009045 (2021).
18. Entezari, M. et al. LncRNA-miRNA axis in tumor progression and therapy response: an emphasis on molecular interactions and therapeutic interventions. *Biomed. Pharmacother.* **154**, 113609. https://doi.org/10.1016/j.biopha.2022.113609 (2022).
19. Robinson, E. K., Covarrubias, S. & Carpenter, S. The how and why of LncRNA function: an innate immune perspective. *Biochim. Biophys. Acta Gene Regul. Mech.* **1863**, 194419. https://doi.org/10.1016/j.bbagrm.2019.194419 (2020).
20. Zhang, Q. et al. A review on the role of long non-coding RNA and microRNA network in clear cell renal cell carcinoma and its tumor microenvironment. *Cancer Cell. Int.* **23**, 16. https://doi.org/10.1186/s12935-023-02861-6 (2023).
21. Statello, L., Guo, C. J., Chen, L. L. & Huarte, M. Gene regulation by long non-coding RNAs and its biological functions. *Nat. Rev. Mol. Cell. Biol.* **22**, 96–118. https://doi.org/10.1038/s41580-020-00315-9 (2021).
22. Gharib, E. et al. IL-2RG as a possible immunotherapeutic target in CRC predicting poor prognosis and regulated by miR-7-5p and miR-26b-5p. *J. Transl Med.* **22**, 439. https://doi.org/10.1186/s12967-024-05251-2 (2024).
23. Tang, Z., Kang, B., Li, C., Chen, T. & Zhang, Z. GEPIA2: an enhanced web server for large-scale expression profiling and interactive analysis. *Nucleic Acids Res.* **47**, W556–w560. https://doi.org/10.1093/nar/gkz430 (2019).
24. Tomczak, K., Czerwińska, P. & Wiznerowicz, M. The cancer genome atlas (TCGA): an immeasurable source of knowledge. *Contemp. Oncol. (Pozn).* **19**, A68–77. https://doi.org/10.5114/wo.2014.47136 (2015).
25. Ritchie, M. E. et al. Limma powers differential expression analyses for RNA-sequencing and microarray studies. *Nucleic Acids Res.* **43**, e47. https://doi.org/10.1093/nar/gkv007 (2015).
26. Bhattacharya, S. et al. ImmPort, toward repurposing of open access immunological assay data for translational and clinical research. *Sci. Data.* **5**, 180015. https://doi.org/10.1038/sdata.2018.15 (2018).
27. Breuer, K. et al. InnateDB: systems biology of innate immunity and beyond–recent updates and continuing curation. *Nucleic Acids Res.* **41**, D1228–1233. https://doi.org/10.1093/nar/gks1147 (2013).
28. Wilkerson, M. D. & Hayes, D. N. ConsensusClusterPlus: a class discovery tool with confidence assessments and item tracking. *Bioinformatics* **26**, 1572–1573. https://doi.org/10.1093/bioinformatics/btq170 (2010).
29. Kanehisa, M., Furumichi, M., Sato, Y., Matsuura, Y. & Ishiguro-Watanabe, M. KEGG: biological systems database as a model of the real world. *Nucleic Acids Res.* **53**, D672–d677. https://doi.org/10.1093/nar/gkae909 (2025).
30. Kanehisa, M. & Goto, S. KEGG: Kyoto encyclopedia of genes and genomes. *Nucleic Acids Res.* **28**, 27–30. https://doi.org/10.1093/nar/28.1.27 (2000).
31. Subramanian, A. et al. Gene set enrichment analysis: a knowledge-based approach for interpreting genome-wide expression profiles. *Proc. Natl. Acad. Sci. U S A.* **102**, 15545–15550. https://doi.org/10.1073/pnas.0506580102 (2005).
32. Hänzelmann, S., Castelo, R. & Guinney, J. GSVA: gene set variation analysis for microarray and RNA-seq data. *BMC Bioinform.* **14**, 7. https://doi.org/10.1186/1471-2105-14-7 (2013).
33. Yoshihara, K. et al. Inferring tumour purity and stromal and immune cell admixture from expression data. *Nat. Commun.* **4**, 2612. https://doi.org/10.1038/ncomms3612 (2013).
34. Han, Y. et al. TISCH2: expanded datasets and new tools for single-cell transcriptome analyses of the tumor microenvironment. *Nucleic Acids Res.* **51**, D1425–d1431. https://doi.org/10.1093/nar/gkac959 (2023).
35. Geeleher, P., Cox, N. & Huang, R. S. pRRophetic: an R package for prediction of clinical chemotherapeutic response from tumor gene expression levels. *PLoS One.* **9**, e107468. https://doi.org/10.1371/journal.pone.0107468 (2014).
36. Wettersten, H. I., Aboud, O. A., Lara, P. N. Jr. & Weiss, R. H. Metabolic reprogramming in clear cell renal cell carcinoma. *Nat. Rev. Nephrol.* **13**, 410–419. https://doi.org/10.1038/nrneph.2017.59 (2017).
37. Ferlay, J. et al. Cancer incidence and mortality patterns in Europe: estimates for 40 countries and 25 major cancers in 2018. *Eur. J. Cancer.* **103**, 356–387. https://doi.org/10.1016/j.ejca.2018.07.005 (2018).
38. de Visser, K. E. & Joyce, J. A. The evolving tumor microenvironment: from cancer initiation to metastatic outgrowth. *Cancer Cell.* **41**, 374–403. https://doi.org/10.1016/j.ccell.2023.02.016 (2023).
39. Zhang, M. et al. Selective targeting of JAK/STAT signaling is potentiated by Bcl-xL blockade in IL-2-dependent adult T-cell leukemia. *Proc. Natl. Acad. Sci. U S A.* **112**, 12480–12485. https://doi.org/10.1073/pnas.1516208112 (2015).
40. Le Floc'h, A. et al. Blocking common γ chain cytokine signaling ameliorates T cell-mediated pathogenesis in disease models. *Sci. Transl Med.* **15**, eabo0205. https://doi.org/10.1126/scitranslmed.abo0205 (2023).
41. Kalman, L. et al. Mutations in genes required for T-cell development: IL7R, CD45, IL2RG, JAK3, RAG1, RAG2, ARTEMIS, and ADA and severe combined immunodeficiency: huge review. *Genet. Med.* **6**, 16–26. https://doi.org/10.1097/01.Gim.0000105752.80592.A3 (2004).
42. Schreiber, R. D., Old, L. J. & Smyth, M. J. Cancer immunoediting: integrating immunity's roles in cancer suppression and promotion. *Science* **331**, 1565–1570. https://doi.org/10.1126/science.1203486 (2011).
43. Qin, H. et al. Integration of ubiquitination-related genes in predictive signatures for prognosis and immunotherapy response in sarcoma. *Front. Oncol.* **14**, 1446522. https://doi.org/10.3389/fonc.2024.1446522 (2024).
44. Zhou, Z. et al. Identification and validation of a Ferroptosis-Related long Non-Coding RNA (FRlncRNA) signature to predict survival outcomes and the immune microenvironment in patients with clear cell renal cell carcinoma. *Front. Genet.* **13**, 787884. https://doi.org/10.3389/fgene.2022.787884 (2022).
45. Liu, L. et al. Bioinformatics analysis of markers based on m(6) A related to prognosis combined with immune invasion of renal clear cell carcinoma. *Cell. Biol. Int.* **47**, 260–272. https://doi.org/10.1002/cbin.11929 (2023).
46. Xue, Q. et al. Construction of a prognostic immune-related LncRNA model and identification of the immune microenvironment in middle- or advanced-stage lung squamous carcinoma patients. *Heliyon* **8**, e09521. https://doi.org/10.1016/j.heliyon.2022.e09521 (2022).
47. Chen, C. & Zheng, H. LncRNA LINC00944 promotes tumorigenesis but suppresses Akt phosphorylation in renal cell carcinoma. *Front. Mol. Biosci.* **8**, 697962. https://doi.org/10.3389/fmolb.2021.697962 (2021).
48. de Santiago, P. R. et al. Immune-related lncRNA LINC00944 responds to variations in ADAR1 levels and it is associated with breast cancer prognosis. *Life Sci.* **268**, 118956. https://doi.org/10.1016/j.lfs.2020.118956 (2021).
49. Wu, L. et al. A novel cuproptosis-related LncRNAs signature predicts prognosis in bladder cancer. *Aging (Albany NY).* **15**, 6445–6466. https://doi.org/10.18632/aging.204861 (2023).
50. Lai, J., Miao, S. & Ran, L. Ferroptosis-associated LncRNA prognostic signature predicts prognosis and immune response in clear cell renal cell carcinoma. *Sci. Rep.* **13**, 2114. https://doi.org/10.1038/s41598-023-29305-5 (2023).
51. Zhang, X. et al. Long non-coding RNA LINC02446 suppresses the proliferation and metastasis of bladder cancer cells by binding with EIF3G and regulating the mTOR signalling pathway. *Cancer Gene Ther.* **28**, 1376–1389. https://doi.org/10.1038/s41417-020-00285-2 (2021).

52. Enguita, F. J. et al. The interplay between lncrnas, RNA-binding proteins and viral genome during SARS-CoV-2 infection reveals strong connections with regulatory events involved in RNA metabolism and immune response. *Theranostics* **12**, 3946–3962. https://doi.org/10.7150/thno.73268 (2022).
53. Tong, H. et al. An epithelial-mesenchymal transition-related long noncoding RNA signature correlates with the prognosis and progression in patients with bladder cancer. *Biosci. Rep.* **41** https://doi.org/10.1042/bsr20203944 (2021).
54. Liu, J., Geng, X., Hou, J. & Wu, G. New insights into M1/M2 macrophages: key modulators in cancer progression. *Cancer Cell. Int.* **21**, 389. https://doi.org/10.1186/s12935-021-02089-2 (2021).
55. Kumar, V. & Barrett, J. E. Toll-Like receptors (TLRs) in health and disease: an overview. *Handb. Exp. Pharmacol.* **276**, 1–21. https://doi.org/10.1007/164_2021_568 (2022).
56. Laletin, V., Bernard, P. L., da Silva, C., Guittard, C., Nunes, J. A. & G. & Negative intracellular regulators of T-cell receptor (TCR) signaling as potential antitumor immunotherapy targets. *J. Immunother Cancer*. **11** https://doi.org/10.1136/jitc-2022-005845 (2023).
57. Villar, V. H. et al. Transforming growth Factor-β1 in cancer immunology: opportunities for immunotherapy. *Adv. Exp. Med. Biol.* **1408**, 309–328. https://doi.org/10.1007/978-3-031-26163-3_17 (2023).
58. Wu, X. et al. Integrated analysis of glutathione metabolic pathway in pancreatic cancer. *Front. Cell. Dev. Biol.* **10**, 896136. https://doi.org/10.3389/fcell.2022.896136 (2022).
59. Whiteside, T. L. Immune suppression in cancer: effects on immune cells, mechanisms and future therapeutic intervention. *Semin Cancer Biol.* **16**, 3–15. https://doi.org/10.1016/j.semcancer.2005.07.008 (2006).
60. Boutilier, A. J. & Elsawa, S. F. Macrophage polarization states in the tumor microenvironment. *Int. J. Mol. Sci.* **22** https://doi.org/10.3390/ijms22136995 (2021).
61. Li, M. et al. Metabolism, metabolites, and macrophages in cancer. *J. Hematol. Oncol.* **16**, 80. https://doi.org/10.1186/s13045-023-01478-6 (2023).
62. Gonçalves, A. C. et al. Impact of cancer metabolism on therapy resistance—clinical implications. *Drug Resist. Updat.* **59**, 100797. https://doi.org/10.1016/j.drup.2021.100797 (2021).
63. Eggenhuizen, P. J., Ng, B. H. & Ooi, J. D. Treg enhancing therapies to treat autoimmune diseases. *Int. J. Mol. Sci.* **21** https://doi.org/10.3390/ijms21197015 (2020).
64. Domagala, M. et al. Cancer cells resistance shaping by tumor infiltrating myeloid cells. *Cancers (Basel)*. 13. https://doi.org/10.3390/cancers13020165 (2021).
65. Sun, Y. et al. ZDHHC2-Mediated AGK palmitoylation activates AKT-mTOR signaling to reduce Sunitinib sensitivity in renal cell carcinoma. *Cancer Res.* **83**, 2034–2051. https://doi.org/10.1158/0008-5472.Can-22-3105 (2023).
66. Fernández-Pello, S. et al. A systematic review and Meta-analysis comparing the effectiveness and adverse effects of different systemic treatments for Non-clear cell renal cell carcinoma. *Eur. Urol.* **71**, 426–436. https://doi.org/10.1016/j.eururo.2016.11.020 (2017).
67. Wood, C. G. et al. Neoadjuvant pazopanib and molecular analysis of tissue response in renal cell carcinoma. *JCI Insight*. **5** https://doi.org/10.1172/jci.insight.132852 (2020).
68. Zhuang, T. Z. et al. Metastatic clear-cell renal cell carcinoma in the era of immune checkpoint inhibitors: therapies and ongoing trials. *Cancers (Basel)*. 14. https://doi.org/10.3390/cancers14122867 (2022).
69. Roskoski, R. Jr Combination immune checkpoint and targeted protein kinase inhibitors for the treatment of renal cell carcinomas. *Pharmacol. Res.* **203**, 107181. https://doi.org/10.1016/j.phrs.2024.107181 (2024).
70. Ali, E. S. et al. Recent advances and limitations of mTOR inhibitors in the treatment of cancer. *Cancer Cell. Int.* **22**, 284. https://doi.org/10.1186/s12935-022-02706-8 (2022).
71. Li, C. et al. Sorafenib enhanced the function of myeloid-derived suppressor cells in hepatocellular carcinoma by facilitating PPARα-mediated fatty acid oxidation. *Mol. Cancer*. **24**, 34. https://doi.org/10.1186/s12943-025-02238-5 (2025).
72. Jin, J. et al. Sunitinib resistance in renal cell carcinoma: from molecular mechanisms to predictive biomarkers. *Drug Resist. Updat.* **67**, 100929. https://doi.org/10.1016/j.drup.2023.100929 (2023).
73. Panwar, V. et al. Multifaceted role of mTOR (mammalian target of rapamycin) signaling pathway in human health and disease. *Signal. Transduct. Target. Ther.* **8**, 375. https://doi.org/10.1038/s41392-023-01608-z (2023).
74. Gril, B. et al. Pazopanib reveals a role for tumor cell B-Raf in the prevention of HER2 + breast cancer brain metastasis. *Clin. Cancer Res.* **17**, 142–153. https://doi.org/10.1158/1078-0432.Ccr-10-1603 (2011).
75. Dahiya, M. & Dureja, H. Sorafenib for hepatocellular carcinoma: potential molecular targets and resistance mechanisms. *J. Chemother.* **34**, 286–301. https://doi.org/10.1080/1120009x.2021.1955202 (2022).
76. Hua, S. et al. Identification and validation of an immune-related gene prognostic signature for clear cell renal carcinoma. *Front. Immunol.* **13**, 869297. https://doi.org/10.3389/fimmu.2022.869297 (2022).
77. Xia, Q. D. et al. Identification of a twelve epithelial-mesenchymal transition-related LncRNA prognostic signature in kidney clear cell carcinoma. *Dis. Markers*. **2022** (8131007). https://doi.org/10.1155/2022/8131007 (2022).
78. Farias, E., Terrematte, P. & Stransky, B. Machine learning gene signature to metastatic CcRCC based on CeRNA network. *Int. J. Mol. Sci.* **25** https://doi.org/10.3390/ijms25084214 (2024).
79. Wang, G. et al. Novel prognosis and therapeutic response model of immune-related LncRNA pairs in clear cell renal cell carcinoma. *Vaccines (Basel)*. 10. https://doi.org/10.3390/vaccines10071161 (2022).
80. Liu, H. et al. A panel of Four-lncRNA signature as a potential biomarker for predicting survival in clear cell renal cell carcinoma. *J. Cancer*. **11**, 4274–4283. https://doi.org/10.7150/jca.40421 (2020).
81. Gu, J., Zhang, X., Peng, Z., Peng, Z. & Liao, Z. A novel immune-related gene signature for predicting immunotherapy outcomes and survival in clear cell renal cell carcinoma. *Sci. Rep.* **13**, 18922. https://doi.org/10.1038/s41598-023-45966-8 (2023).

Author contributions

WJ H: writing—original draft, conceptualization, methodology, validation; BW: writing—original draft, conceptualization, methodology, validation; YQ C: conceptualization, software; XL G: investigation; XS W: investigation; DW W: resources, project administration, writing—review & editing, supervision, project administration.

Funding

This work was supported by the Beijing Bethune Charitable Foundation, Special Research Fund for Urological Oncology [Grant Numbers mnzl202029]; the Research Project Supported by Shanxi Scholarship Council of China[grant number [2021–160].

Declarations

Competing interests

The authors declare no competing interests.

Informed consent

Informed consent was obtained from all subjects involved in the study.

Institutional review board statement

The study was conducted in accordance with the Declaration of Helsinki, and approved by the Ethics Committee of the First Hospital of Shanxi Medical University (No.2021K034,2021-04-26).

Additional information

Supplementary Information The online version contains supplementary material available at https://doi.org/10.1038/s41598-025-15439-1.

Correspondence and requests for materials should be addressed to D.W.

Reprints and permissions information is available at www.nature.com/reprints.

Publisher's note Springer Nature remains neutral with regard to jurisdictional claims in published maps and institutional affiliations.